

AD-A257 627



2

# NAVAL POSTGRADUATE SCHOOL

## Monterey, California



DTIC  
ELECTE  
DEC 01 1992  
S E D

### THESIS

SUN SENSOR IMPLEMENTATION  
USING SOLAR POWER ARRAYS

by

Irma Sityar  
September 1992

Thesis Advisor:

Randy L. Wight

Approved for public release; distribution is unlimited

92-30496

Unclassified

Security Classification of this page

## REPORT DOCUMENTATION PAGE

1a Report Security Classification <b>Unclassified</b>			1b Restrictive Markings														
2a Security Classification Authority			3 Distribution Availability of Report <b>Approved for public release; distribution is unlimited.</b>														
2b Declassification/Downgrading Schedule			5 Monitoring Organization Report Number(s)														
4 Performing Organization Report Number(s)			7a Name of Monitoring Organization <b>Naval Postgraduate School</b>														
6a Name of Performing Organization <b>Naval Postgraduate School</b>		6b Office Symbol (If Applicable) <b>32</b>	7b Address (city, state, and ZIP code) <b>Monterey, CA 93943-5000</b>														
6c Address (city, state, and ZIP code) <b>Monterey, CA 93943-5000</b>		9 Procurement Instrument Identification Number															
8a Name of Funding/Sponsoring Organization		8b Office Symbol (If Applicable)	10 Source of Funding Numbers														
8c Address (city, state, and ZIP code)		<table border="1"> <tr> <td>Program</td> <td>Element Number</td> <td>Project No</td> <td>Task No</td> <td>Work Unit</td> <td>Accession No</td> </tr> <tr> <td></td> <td></td> <td></td> <td></td> <td></td> <td></td> </tr> </table>				Program	Element Number	Project No	Task No	Work Unit	Accession No						
Program	Element Number	Project No	Task No	Work Unit	Accession No												
11 Title (Include Security Classification) <b>SUN SENSOR IMPLEMENTATION USING SOLAR POWER ARRAYS</b>																	
12 Personal Author(s) <b>Irma Sityar</b>																	
13a Type of Report <b>Master's Thesis</b>		13b Time Covered From To		14 Date of Report (year, month, day) <b>September 1992</b>													
				15 Page Count <b>82</b>													
16 Supplementary Notation <b>The views expressed in this thesis are those of the author and do not reflect the official policy or position of the Department of Defense or the U.S. Government.</b>																	
17 Cosati Codes			18 Subject Terms (continue on reverse if necessary and identify by block number)														
Field	Group	Subgroup	Sun Sensor, Space Electrical Power Systems, PANSAT Satellite, Solar Cells														
19 Abstract (continue on reverse if necessary and identify by block number)																	
<p>This thesis explores the feasibility of utilizing a satellite's solar cell power arrays as a sun sensor. Power output of a solar cell is highly dependent on the intensity and direction of sunlight that falls on the panel and thus provides an indication of the sun's orientation. A sun sensor can be obtained by processing the power signal generated in each solar cell panel.</p> <p>This concept was applied to the Navel Postgraduate School's Petite Amateur Navy Satellite (PANSAT), a 26 sided polyhedral shaped satellite with 17 body mounted square panels. Two circuit configurations to meter the power signals generated in the 17 individual solar panels were investigated. It was possible in one configuration to develop a prediction model of each panel's short circuit current versus sun angle. Compensation for seasonal variations in solar flux, solar cell degradation due to radiation and panel temperature variation is required. An estimation of the resulting sun sensor's resolution and accuracy is given.</p>																	
20 Distribution/Availability of Abstract			21 Abstract Security Classification														
<input checked="" type="checkbox"/> unclassified/unlimited <input type="checkbox"/> same as report <input type="checkbox"/> DTIC users			<b>Unclassified</b>														
22a Name of Responsible Individual <b>Randy L. Wight, CDR</b>			22b Telephone (Include Area code) <b>(408) 646-3403</b>		22c Office Symbol <b>SP/Wt</b>												

DD FORM 1473, 84 MAR

83 APR edition may be used until exhausted

All other editions are obsolete

security classification of this page

Unclassified

Approved for public release; distribution is unlimited.

**Sun Sensor Implementation Using  
Solar Power Arrays**

by

**Irma Sityar  
Lieutenant, United States Navy  
B.S., The Cooper Union , 1983**

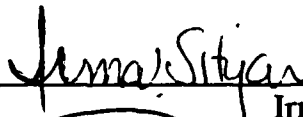
**Submitted in partial fulfillment of the  
requirements for the degree of**

**MASTER OF SCIENCE IN ELECTRICAL ENGINEERING**

from the

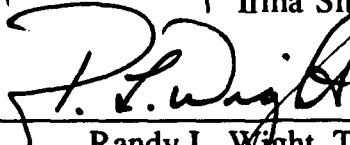
**NAVAL POSTGRADUATE SCHOOL  
September 1992**

Author:

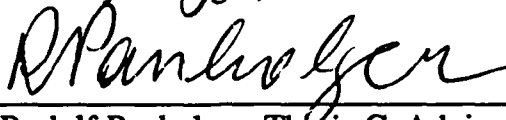


Irma Sityar

Approved by:



Randy L. Wight, Thesis Advisor



Rudolf Panholzer, Thesis CoAdvisor



Edward Euler, Second Reader



Michael A. Morgan, Chairman,  
Department of Electrical and Computer Engineering

## ABSTRACT

This thesis explores the feasibility of utilizing a satellite's solar cell power arrays as a sun sensor. Power output of a solar cell is highly dependent on the intensity and direction of sunlight that falls on the panel and thus provides an indication of the sun's orientation. A sun sensor can be obtained by processing the power signal generated in each solar cell panel.

This concept was applied to the Naval Postgraduate School's Petite Amateur Navy Satellite (PANSAT), a 26 sided polyhedral shaped satellite with 17 body mounted square solar panels. Two circuit configurations to meter the power signals generated in the 17 individual solar panels were investigated. It was possible in one configuration to develop a prediction model of each panel's short circuit current versus sun angle. Compensation for seasonal variations in solar flux, solar cell degradation due to radiation and panel temperature variation is required. An estimation of the resulting sun sensor's resolution and accuracy is given.

Accession For	
NTIS CRA&I	<input checked="checked" type="checkbox"/>
DTIC TAB	<input type="checkbox"/>
Unannounced	<input type="checkbox"/>
Justification .....	
By .....	
Distribution / .....	
Availability Codes	
Dist	Avail and/or Special
A-1	

NOT REPLY INSPECTED 2

## TABLE OF CONTENTS

I. INTRODUCTION .....	1
A. PURPOSE .....	1
B. SOLAR CELL DEVELOPMENT .....	2
1. Non Silicon Solar Cell Development .....	4
C. OVERVIEW .....	5
II. SOLAR CELL THEORY .....	6
A. SEMICONDUCTOR PROPERTIES .....	6
B. SOLAR CELL OPERATION .....	7
C. SOLAR CELL PARAMETERS .....	10
D. NON IDEAL SOLAR CELL .....	13
III. SOLAR CELLS AS POWER ELEMENTS .....	15
A. SOLAR CELL ARRAY .....	15
1. Optical Subsystem .....	15
2. Electrical Subsystem .....	17
a. Interconnectors .....	17
b. Diodes .....	18
3. Mechanical Subsystem .....	20
B. ARRAY DESIGN CRITERIA .....	23

C. ARRAY SIZING CALCULATIONS .....	29
1. Maximum Power Output (EOL) .....	29
2. Voltage Level (EOL) .....	30
3. Load Current .....	31
4. Reverse Bias Solar Cells .....	32
IV. SPACE ELECTRICAL POWER SYSTEMS .....	35
A. POWER SYSTEM COMPONENTS .....	35
1. Power Conditioning Unit .....	35
2. Battery .....	37
3. Load Profile .....	40
B. SYSTEM INTEGRATION .....	41
C. PANSAT ELECTRICAL POWER SYSTEM .....	42
V. SUN SENSORS .....	50
A. ANALOG SUN SENSORS .....	50
B. DIGITAL SUN SENSORS .....	51
C. PANSAT SUN SENSOR IMPLEMENTATION .....	57
1. Shunt Method .....	57
a. Resolution .....	59
b. Accuracy .....	59
c. Sampling Frequency .....	60

2. Series Method .....	61
V. CONCLUSIONS .....	64
APPENDIX A - RESOLUTION CALCULATION .....	67
APPENDIX B - SHUNT METHOD PREDICTION PROGRAM .....	69
LIST OF REFERENCES .....	73
INITIAL DISTRIBUTION LIST .....	75

## **I. INTRODUCTION**

### **A. PURPOSE**

Solar cells have been predominately used for electric power generation. They are also used in various applications as light detectors. The design considerations that influence systems that utilize solar cells as power elements differ from those that utilize them as electro-optical sensors. Thus configurations that optimize a solar cell's performance in one application may degrade its performance in a different application.

This thesis explores the feasibility of utilizing a satellite's solar cell power arrays as a sun sensor. Power output of a solar cell is highly dependent on the intensity and direction of sunlight that falls on the panel and thus provides an indication of the sun's orientation. A sun sensor can be obtained by processing the power signal generated in each solar cell panel.

This concept was applied to the Naval Postgraduate School's Petite Amateur Navy Satellite (PANSAT), a 26 sided polyhedral shaped satellite with 17 body mounted square solar panels. Two circuit configurations to meter the power signals generated in the 17 individual solar panels were investigated. It was possible in one configuration to develop a prediction model of each panel's short circuit current versus sun angle. Compensation for seasonal variations in solar flux, solar cell degradation due to radiation and panel temperature variation is required. An estimation of the resulting sun sensor's resolution and accuracy is given.



## **B. SOLAR CELL DEVELOPMENT**

Solar cells are devices which convert solar energy into electrical energy. This is accomplished through the photovoltaic effect. Photovoltaic energy conversion is based on a quantum mechanical process by which incident photons free charge carriers from their normally bound conditions within a semiconductor. [Ref. 1:p. 1.2-1]

The recorded beginning of photovoltaic research dates back to 1839, when Becquerel published his work on photoelectric experimentation with acidic aqueous solutions and noble metal electrodes. The first work on solid-state photovoltaic devices was reported in 1876. [Ref. 2:p. 156] Suitable materials for achieving a photovoltaic effect are inherently limited to those with a conduction band energy gap slightly less than the energy of the photon radiation.

Commercial exploitation, first of photoconductive and later of photovoltaic selenium cells began about 1880 and has continued through today. Intensive research conducted on selenium, copper oxide and many other semiconductor compounds / metal oxide type barrier devices during the 1920's and 1930's provided the foundations for the theoretical understanding of photovoltaic potential barrier solar cells and their mathematical modeling. During the late 1930's and early 1940's intensive semiconductor material research focused on germanium and silicon. This effort resulted in the development of the transistor and of the silicon solar cell. [Ref. 2:p. 156]

The first practical solar cells were developed in 1954 by the Bell Telephone Laboratories. This cell was of the planar junction, single crystal silicon n-type and were initially considered for terrestrial use only. The first solar cell array that successfully operated in space was launched on March 17, 1958, on board

Vanguard I, the second United States earth satellite. This solar cell array consisted of six solar cell panels distributed over and mounted to the outer surface of an approximately spherical spacecraft body. Each panel was made of 18 n-type solar cells measuring  $2 \times 0.5$  cm size with an energy conversion efficiency of approximately ten percent at  $28^{\circ}\text{C}$ . This solar array system provided less than one watt of power for more than six years. [Ref. 2:p. 8]

Solar cells are especially suited for space applications because they require no fuel, thus saving payload. Theoretically, they can provide an almost inexhaustible supply of power without emitting radiation or waste by-products. Most satellites and space vehicles launched to date have utilized solar cell energy as their main source of power.

Solar cells initially produced in the United States were n-type silicon ( p-type layer diffused onto a n-type silicon substrate ). It was later found that cells made from p-type silicon ( n-type layer diffused onto a p-type silicon substrate ) were more resistant to irradiation with electrons, protons , neutrons and other particles found in space. After 1960 solar cell production switched over to p-type silicon. [Ref. 2:p. 156 ]

Solar cell producers have adapted concurrent advances in the semiconductor industry to provide improved cell performance. Space solar technology has steadily improved. As a result cell efficiency has doubled ( 8% to 16%) for silicon cells and is around 20% for gallium arsenide (GaAs) cells. Cell sizes have increased thirty-fold. They are now approaching 100 square centimeters. [Ref. 3:p. 76]

Currently the most common solar cell is the single crystal silicon solar cell which has a typical maximum energy conversion efficiency of 10 to 14 percent at

25°C under air-mass zero conditions ( i.e. the absence of any atmospheric attenuation or filtering of the sun's radiation, denoted as "AM0"). This corresponds to an electrical output of about 15 to 20 mW/cm<sup>2</sup> at approximately 0.45 volts. [Ref. 1:p. 1.2-1] Various exotic silicon cell designs have been tested for special applications including textured surface cells which have a slightly higher power output and can operate at higher temperatures.

### **1. Non-Silicon Solar Cell Development**

Silicon has been the workhorse material for solar cells. However the advantages of GaAs cells, namely 25% higher efficiency, lower loss of output at higher temperatures and increased radiation resistance have recently become important enough to justify its higher expense for some applications.

The use of germanium (Ge) as a substrate for GaAs has been recently developed. This takes advantage of the superior mechanical properties of Ge. Ge is closely matched to GaAs in atomic lattice spacing and in thermal expansion coefficient. High efficiency GaAs cells grown on Ge substrates and thinned to around 100 micrometers retain good mechanical strength. This offsets the increased weight resulting from the high density of GaAs and the mechanical problems in handling thin GaAs slices. The GaAs/Ge cell structure has been extended to include an active junction at the GaAs/Ge interface. This has resulted in cascade cells with the promise of efficiencies up to 25%. [Ref. 3:p. 77]

Highly efficient solar cells have been made from indium phosphide (InP) . These cells have an additional advantage - the ability to recover from radiation damage through annealing while operating at ambient temperatures. GaAs cells need temperatures around 150°C to 250°C for annealing to occur while most silicon cells do not anneal at temperatures below 450°C. InP cells offer an

attractive alternative for space missions where high radiation damage is expected.

[Ref. 3:p. 77]

Though the exact solar cell array type to be used in PANSAT has not yet been finalized, it is expected that standard silicon cells will be utilized. As a result this thesis focused entirely on the performance characteristics of silicon solar cells.

### **C. OVERVIEW**

The basics of solar cell theory is presented in Chapter II. The terminal parameters which describe a solar cell,  $I_{SC}$  (short circuit current),  $V_{OC}$  (open circuit voltage),  $I_{mp}$  (current at maximum power) and  $V_{mp}$  (voltage at maximum power) are defined.

In Chapters III and IV, the concerns of an electrical power system designer are presented. Chapter III describes how solar cells are configured to provide the required power. Different electrical power system topologies are explained in Chapter IV.

Chapter V focuses on how solar cells can be utilized as sun sensor elements. The two basic types of commercially available sun sensors are analyzed. Two ways to implement a sun sensor within an electrical power system are then presented. Evaluation of the resulting sun sensor and its impact on the electrical power system performance is presented in Chapter VI.

## **II. SOLAR CELL THEORY**

### **A. SEMICONDUCTOR PROPERTIES**

Semiconductors such as silicone, are unique in that current flow is due to both the motion of electrons in the conduction band and the effective motion of vacancies or holes in the valence band. There are two mechanisms by which holes and electrons move through a semiconductor crystal - drift and diffusion. Carrier drift occurs when an electric field is applied across the semiconductor. The resulting movement of electrons and holes create a drift current. Diffusion is associated with random movement due to thermal ionization. With uniform concentrations of free electrons and holes this random motion does not result in a net flow of charge. However if the electron or hole concentration were higher in one region of the crystal, the charge from that region would tend to move toward other regions with lower concentration. This gives rise to a diffusion current. [Ref. 4:p. 186]

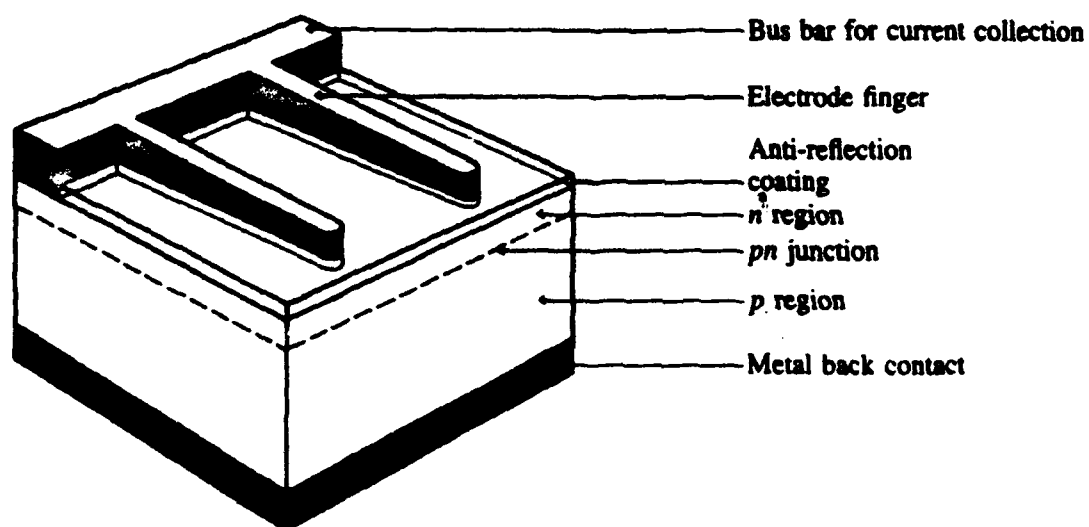
An intrinsic semiconductor is one in which the free electrons in the conduction band and the free holes in the valence band are due solely to thermal ionization. Extrinsic semiconductors are materials in which carriers of one kind (electrons or holes ) predominate. This is done by introducing specialized impurities known as dopants which donate or accept electrons from the semiconductor thereby enhancing carrier conduction of one type. The majority of the charge carriers are electrons in an n-type semiconductor while for a p-type, the majority of charge carriers are holes.

## B. SOLAR CELL OPERATION

Silicone solar cells are two terminal devices formed by creating regions of different doping, thus creating a pn junction. (See Figure 2-1.) Because of the difference in the electron and hole concentrations between the two sides of the junction, there is a strong tendency for electrons to diffuse from the n-side to the p-side and for the holes to diffuse in the opposite direction. These diffusing charge carriers will quickly recombine once across the junction. This creates a carrier depletion region at the junction. There is also a resulting charge imbalance within each region with the n-side of the junction being positively charged and the p-side being negatively charged. The charge on both sides of the depletion region produces an internal electric field which acts as a barrier opposing further diffusion of holes into the n-region and electrons into the p-region.

In sunlight, the solar cell absorbs incident photons with energy greater than its band gap energy (1.1 eV for silicone). This absorbed energy raises a valence band electron to the conduction band and creates an electron-hole pair. The purpose of the pn junction is to separate and collect the electron hole pairs that are generated. Electrons appearing in the depletion region will be accelerated to the n-region contact while holes appearing in the depletion region will be accelerated to the p-region contact.

Since the depletion region is very narrow, only a small fraction of the electron hole pairs generated by incident photons are produced in this region. Most electron hole pairs are produced in the bulk material unaffected by this junction field. Minority carriers which do reach the junction will most likely recombine after living for a time  $\tau$ , called the lifetime. The distance traveled in time  $\tau$  is called the diffusion length and is given by



Schematic view of typical commercial single-crystal silicon solar cell.

FIGURE 2-1. Silicon Solar Cell PN Junction [Ref. 5:p. 70]

$$L = \sqrt{D\tau} \quad (2-1)$$

where

$D$  = minority carrier diffusion constant.

The depletion region and the generally much larger volume of material lying within a diffusion length on both sides of the depletion region is the active collection region of a pn junction solar cell. [Ref. 6:p. 1-4]

Light generated current  $I_L$ , of a solar cell is formed from minority carrier movement into the depletion region.  $I_L$  is proportional not only to the intensity of the sunlight but also proportional to the cosine of the angle of incidence of the sun's rays. The angle of incidence affects the path distance that the photons have to travel into the solar cell's active region. The shortest distance is at normal incidence ( $\theta = 0^\circ$ ) and increases as  $\theta$  varies from  $0^\circ$  to  $90^\circ$ . At  $\theta = 90^\circ$ , photons do not penetrate into the solar cell and current cannot be generated.

Recombination of minority carriers reduces the current output of the solar cell, thus efforts to increase  $\tau$  and  $L$  will improve solar cell performance. Defects along with any unwanted impurities or other disruptions reduces the diffusion length. Electron, proton, neutron or gamma ray irradiation will produce defect sites in the cell's crystalline structure. After irradiation, the cell's response to red light decreases significantly. The blue response of the solar cell is not affected as much since blue light produces its electron-hole pairs very close to the junction. As a result techniques which enhances the blue response of the solar cell (such as coverglass coatings to increase blue light adsorption) create a more radiation resistant cell. [Ref. 6:p. 1-5]



### C. SOLAR CELL PARAMETERS

In the dark the solar cell is basically a diode. Current flows if an external electric field is applied such that the p-contact is positive with respect to the n-contact. This diode current  $I_D$  is given by

$$I_D = I_0(e^{qV/kT} - 1) \quad (2-2)$$

where

$q$ = magnitude of an electronic charge  
( $1.602 \times 10^{-19}$  coulombs)

$V$ = potential across cell

$k$ = Boltzman's constant  
( $1.38 \times 10^{-23}$  joules/°Kelvin)

$T$ = temperature in °Kelvin

$\gamma$ = curve fitting constant

$I_0$ = diode saturation current.

An ideal circuit model of the solar cell is drawn in Figure 2-2. The load current is equal to

$$\begin{aligned} I &= I_L - I_D \\ &= I_L - I_0(e^{qV/kT} - 1) \end{aligned} \quad (2-3)$$

When the solar cell is shorted,  $R_L = 0$  and  $V = 0$ . Therefore

$$I_{sc} = I_L \propto S \cos \theta \quad (2-4)$$

where

$I_{sc}$ = short circuit current

$S$  = incident solar intensity

$\theta$  = incidence angle of sun's rays.

$I_{SC}$  is not a strong function of temperature increasing, by less than one percent for every 10°K increase. [Ref. 5:p. 57]

At  $R_L = \infty$ ,  $I = 0$ . The open circuit voltage,  $V_{OC}$ , is given as

$$V_{OC} = \frac{\gamma k T}{q} \ln \left( \frac{I_{SC}}{I_0} + 1 \right) \quad (2-5)$$

where variables are as defined in Equation 2-2. It would seem that  $V_{OC}$  is proportional to temperature and would increase as temperature increases. However this is not the case as the  $I_0$  denominator term in the natural log argument is a very strong function of temperature.  $I_0$  increases as temperature increases, doubling for every 5°K rise in temperature.  $V_{OC}$  decreases approximately 2.5 mV per degree Kelvin. [Ref. 4:p. 157]

Open circuit voltage and short circuit current are parameters of key interest to the sun sensor designer. This is discussed in Chapter V.

Figure 2-3 is a typical I-V characteristic curve for a silicon solar cell. This curve is drawn in the fourth quadrant. It shows two curves, a diode I-V curve and the same curve displaced by  $I_{SC}$ , the current the solar cell generates when illuminated. Of key interest to the electrical power system designer are  $I_{mp}$  and  $V_{mp}$ , the current and voltage at maximum power. The maximum power points vary as a function of illumination intensity and temperature. Peak power tracking is advantageous in that it increases the solar array's power density, thus more loads can be supported or the solar array size can be reduced. This is further discussed in Chapter IV.

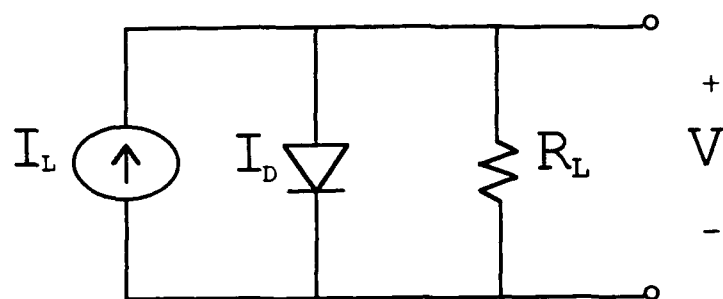
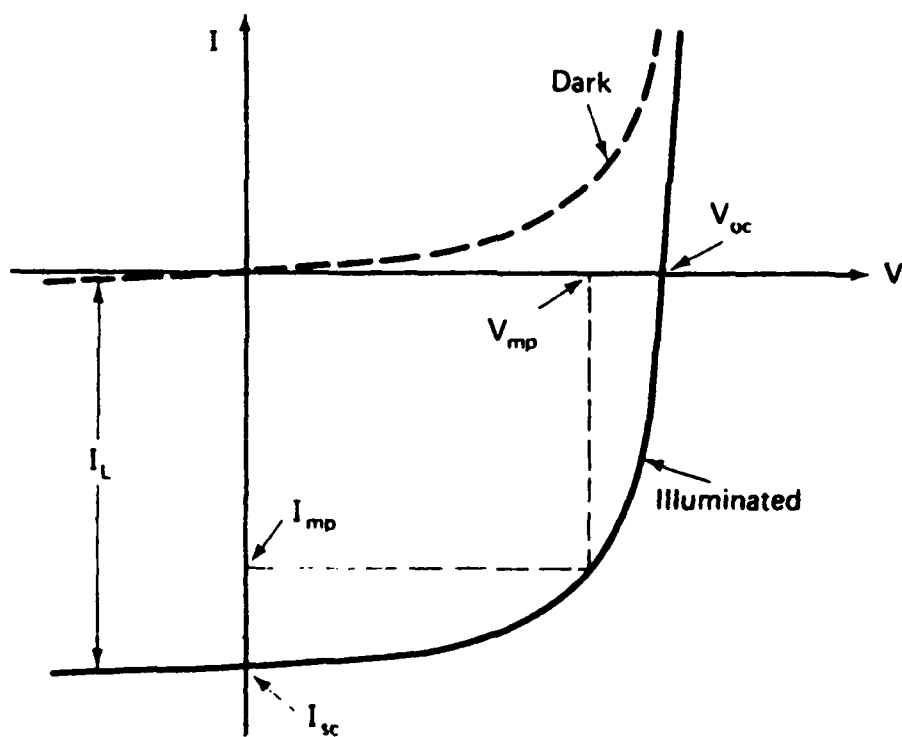


FIGURE 2-2. Ideal Solar Cell Model



Terminal properties of a *p-n* junction diode  
in the dark and when illuminated.

FIGURE 2-3. Solar Cell Terminal Properties [Ref. 7:p. 79]

#### D. NON IDEAL SOLAR CELL

Actual solar cell I-V characteristic curves may deviate from values predicted by Equation 2-3. This is due to losses from parasitic resistances associated with the solar cell. These parasitic resistances are drawn in an equivalent circuit in Figure 2-4. Factors which contribute to the series resistance  $R_S$  are the bulk resistance of the semiconductor making up the cell, the bulk resistance of the metallic contacts and the interconnectors, and the contact resistance between the metallic contacts and the semiconductor. The shunt resistance,  $R_{SH}$ , is caused by leakage across the pn junction around the edge of the cell and in non peripheral regions in the presence of crystal defects and precipitates of foreign impurities in the junction region. Effects of these parasitic resistances are graphed in Figure 2-5. [Ref. 7: p. 96]

The current  $I$ , supplied by the solar cell is given as follows

$$I = I_L - I_o \left[ e^{\left( \frac{q(V + I R_S)}{\gamma k T} \right)} - 1 \right] - \frac{V}{R_{SH}} \quad (2-6)$$

where variables are as previously defined. [Ref. 1: p 9.2-1]

The solar cell model depicted in Figure 2-4 does not predict actual solar cell I-V characteristics with sufficient accuracy for engineering analysis. The parameters  $I_o$ ,  $\gamma$  and  $R_S$  are difficult to measure over all temperature and illumination intensity ranges. Solar array performance obtained empirically are used for calculations in the final design. [Ref. 1: p. 9.2-2]

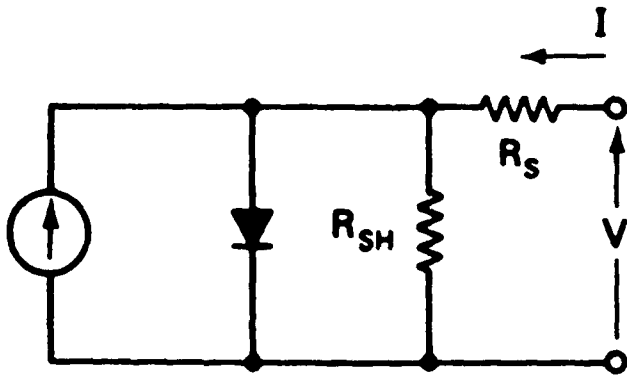
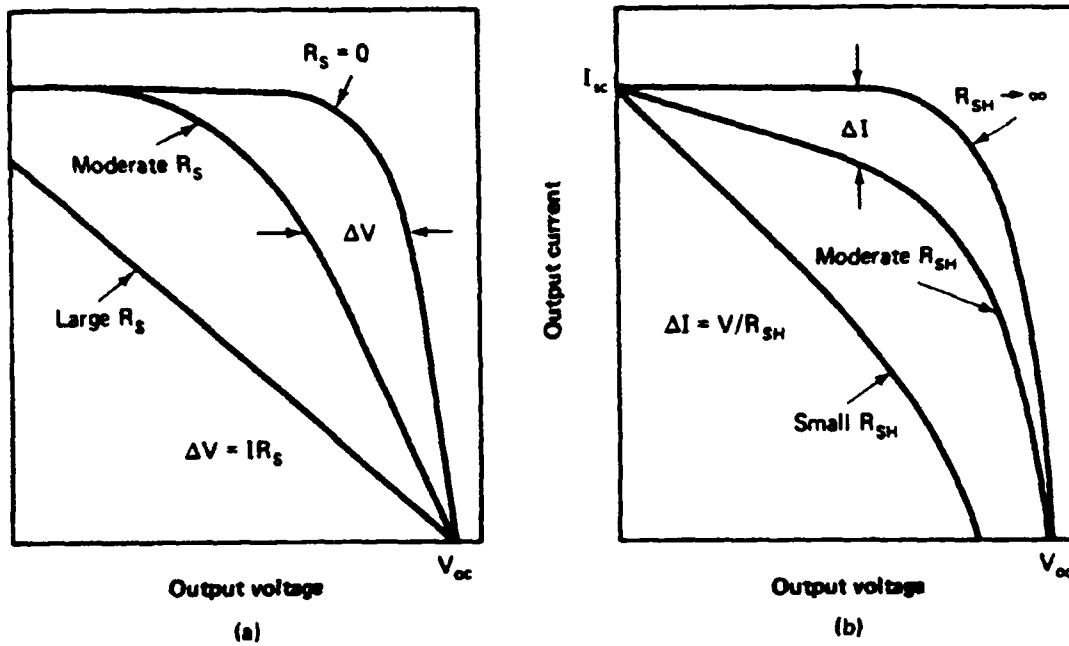


FIGURE 2-4. Non Ideal Solar Cell Model [Ref. 7:p. 95]



Effect of parasitic resistances on the output characteristics of solar cells:

- (a) Effect of series resistance,  $R_S$ .
- (b) Effect of a shunt resistance,  $R_{SH}$ .

FIGURE 2-5. Effect of Parasitic Resistances. [Ref. 7:p. 96]

### **III. SOLAR CELLS AS POWER ELEMENTS**

Solar cells are the basic building blocks which comprise the panels generating the electrical power. They are arranged in arrays. Voltage and current output of the array are determined by the number of cells connected in series and in parallel respectively.

The following sections describe the components that comprise the solar cell array. It discusses how the solar cell is integrated electrically and mechanically into a system to provide the required voltage and current output levels. This background is necessary in order to gain an appreciation for the design considerations involved with using solar cells as a power generating element. Solar cells do not generate high levels of power. End of life average power output for PANSAT is 24.5W. Tremendous design effort is focused on maximizing solar cell efficiency and reducing power losses in the circuit.

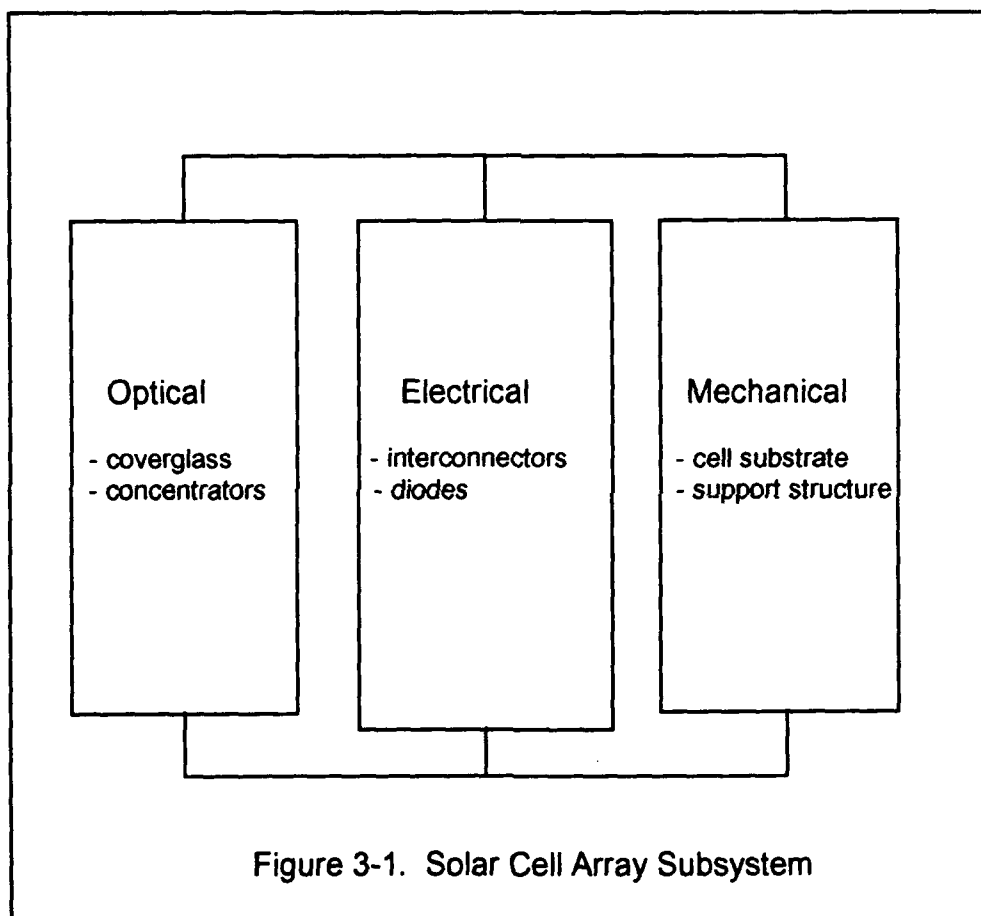
#### **A. SOLAR CELL ARRAY**

The solar cell array can be divided into three subsystem components - optical, electrical and mechanical. These are depicted in Figure 3-1.

##### **1. Optical Subsystem**

The optical subsystem includes the solar cell coverglass and sunlight concentrators (if used). Planar or flat plate arrays (non concentrator type solar cells) utilize transparent covers and thin coatings for the following reasons

- to physically protect solar cells and their electrical connections from environmental hazards



- to minimize losses at the interfaces of optical media having different indices of refraction
- to enhance the amount of sunlight reaching the active portions of solar cells
- to increase the solar cell's heat rejection [Ref. 2:p. 242]

Wavelength selective refraction coatings are used to reflect energy having wavelengths outside the solar cell's range of sensitivity. This decreases the heat input to the solar cell thus lowering the cell's operating temperature. With a lower operating temperature, the cell's operating efficiency is improved.

Sunlight concentrators artificially increase the solar intensity incident on solar cells by means of optical or other devices. Optical concentration devices consist of mirrors (reflectors) , lenses (refractors) or a combination of both. While concentrators increase the amount of sunlight that is usable by the solar cell, it increases the heat input to the cell as well and can adversely affect the cell's efficiency. Concentrator arrays also require fairly accurate sun tracking capability (to within 1.5° to 2°). [Ref. 2:p. 243] Concentrator arrays are not used in PANSAT and were not factored in the sun sensor design.

## **2. Electrical Subsystem**

### ***a. Interconnectors***

The electrical subsystem is comprised of the electrical conductors that connect the solar cells in series and parallel for the required module configuration. These modules are also interconnected into an "electrical string" to provide power output at a bus voltage. The primary design concern is that these circuits be able to provide the required output throughout the defined life of the solar cell. Material selection is based not only on electrical conductivity but on temperature cycling endurance. For space solar cell, temperature cycling



endurance is one of the more difficult requirements to meet. Temperature variations and other external forces stress the solar cell's interconnector assembly which over time can lead to material fatigue and failure. Reliability considerations usually require that a number of redundant current paths be part of the circuit design. [Ref. 2:p. 270]

**b. Diodes**

The electrical subsystem utilizes diodes in three applications. These applications are schematically shown in Figure 3-2.

Blocking diodes (isolation diodes) are inserted between electrical strings of solar cells and the power bus. They conduct current from illuminated solar cell strings to the bus but will block current flow from the bus to the solar cell string should the string voltage fall below the bus voltage.

A non illuminated array behaves as a string of series connected rectifier diodes connected in their forward conduction mode across the power bus. The amount of current that could be drained by a non illuminated array or string of cells without isolation diodes depends on the bus voltage, but typically could range between 0 and 30 percent of the current which the same array would produce when fully illuminated. f. [Ref. 1:p. 5.5-1]

Some power is lost when the diode conducts as the diode's forward voltage drop subtracts from the solar cell array voltage output. The decision to use or not use blocking diodes is based on the tradeoff between power losses by non illuminated cells and power losses in the blocking diodes. This decision is affected by the power level of the solar cell strings, the percentage of non illuminated solar cell strings and the fractional time of non illumination. For spinning body-mounted arrays blocking diodes are almost always essential. [Ref. 1:p. 5.5-1]

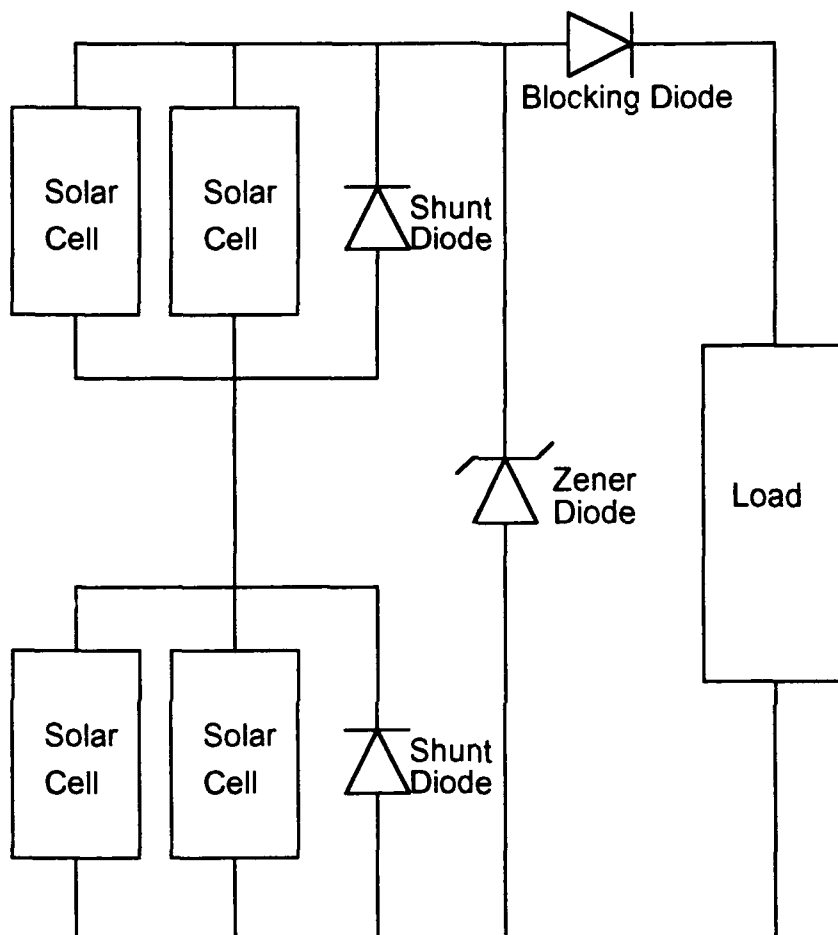


Figure 3-2. Diode Applications

When an individual cell in a string of solar cells becomes shadowed, the shadowed cell can become reverse biased. This phenomenon is further discussed later in this chapter. Cells in parallel with this shadowed cell become reverse biased as well, even if fully illuminated. Reverse biased solar cells can cause permanent short circuit failure, permanent power output loss and excessive localized heating. [ Ref. 8:p. 43]

Shunt diodes are connected across rows of parallel connected solar cell submodules. The shunt diodes are reverse biased when all solar cells are fully illuminated. If a shadowed solar cell submodule becomes reverse biased, the shunt diode will conduct. Shunt diodes are also placed electrically in parallel to solar cells that may undergo higher mechanical stress than other cells in the panel. Thus, if any of these cells crack and completely open, the shunt diode will route current around the damaged cell so that the string can continue to supply power. The voltage output capability of a string of solar cells with an affected submodule is reduced by the voltage that would have been produced by that submodule plus the voltage drop across the shunt diode.

Zener diodes can be used to limit the output voltage of the string thus protecting voltage sensitive loads. They are connected in parallel with the array output terminals. This diode will not conduct unless the string output voltage tries to exceed the zener breakdown voltage  $V_Z$ . When this happens the zener diode will conduct and the string output voltage will be clamped to  $V_Z$ . The power dissipated by the zener diode will generate heat which the solar cell array will absorb. Voltage regulation can be controlled by other electronic means.

### **3. Mechanical Subsystem**

Power output requirements, operating environment considerations and weight and volume limitations are parameters which strongly influence the process

of designing the mechanical support structure of space solar arrays. Substrates are the structural elements that mechanically support and encase the solar cells, cell interconnectors and associated wiring. They are physically located behind the solar cell back sides or in front of the solar cell's active areas. If located in the front of the solar cell they are more correctly called superstrates. Superstrates must be optically transparent.

As a general rule the thinner the substrate the greater the temperature extremes and the lesser the radiation protection. Thus substrate design affects the cell's operating temperature (and therefore efficiency) and resistance to charged particle radiation. [Ref. 1:p. 6.1-2]

Space solar array panels can be divided into two broad structural categories, body mounted panels and deployable panels. Body mounted panels are relatively more straightforward to design. The substrate is an integral part of the satellite body and is typically constructed from sheet/stringer or aluminum sandwich panels. The main disadvantage to body mounted panels are that they have a definite maximum power output limitation. [Ref. 1:p. 6.1-1]

By taking into account such factors as available shroud volume (which dictates maximum satellite size), spin stabilization moment-of-inertia requirements, and space solar cell type, it can be shown that power availability ranges from 50 to 1000 watts. However for satellites requiring more than 200 watts of power, a deployable array is often chosen, especially if three axis stabilization is required by payload or mission. [Ref. 1:p. 6.1-1]

Deployable arrays are inherently more complex because of their moving parts. They are stowed during launch and must successfully unfurl once the satellite is in orbit. Once unfurled, they may have sun tracking mechanisms which

orient the panels toward the sun to maximize the incident solar intensity and thus maximize power output.

Deployable arrays can be flexible or rigid depending on the physical characteristics of the panel substrate. Rigid arrays are mechanically stiffened with a honeycomb structure, usually made of aluminum, sandwiched between two face sheets that provide backside shielding for the solar cells and provide enhanced mechanical support to the structure. The use of an aluminum honeycomb substrate as the primary supporting structure in a space solar array has historically been the preferred approach for DOD and NASA satellites. Rigid arrays have an advantage in that they can provide power to the satellite even while stowed. In addition, the honeycomb substrates are attractive for military satellite platforms with survivability requirements resulting from potential military threats due to their more rugged construction and relatively high area heat capacitance. The disadvantage is their greater weight and volume. [Ref. 9:p. 277]

Flexible arrays are typically a Kapton substrate/superstrate which sandwich the solar cells and electrical circuitry. Two predominant design types are the fold-out array and the roll-out array. The lighter weight flexible array has been utilized for missions with very large power requirements ( greater than 10 kW) such as the Hubble telescope and the Space Station. [Ref. 1:p. 6.1-1]

A variety of concepts have been conceived to create the largest possible solar cell array areas with structural elements that exhibit the lowest weight, highest deployment reliability, and highest possible natural bending frequency (i.e. the highest possible bending stiffness). In practice, solutions to these individual design parameters are in opposition to each other, so that the practical array designs that have evolved are the results of trade studies to optimize each array for a specific mission.[Ref. 2:p. 328]

Several hybrid designs combining body mounted panels and deployable rigid and flexible arrays have had success.

There are also efforts to standardize solar cell arrays so that one configuration could possibly serve various space missions. Solar cells are significant cost items. The benefits of standardized components in terms of economy, resource allocation, technical performance, reliability (through uniformity of product) are well known. Ironically, the major obstacle to such standardization is related to the cost of the launch vehicle. Usually the lowest cost/performance is chosen forcing stringent weight and high operating efficiency constraints on the spacecraft/payload. The economic penalty paid for an optimized array design over a standardized array design is small relative to the cost for a more powerful launch vehicle. [Ref. 1:p. 1.4-1]

Data base of actual lifetime performance exist for a number of solar cell array designs. These proven designs are usually selected as a baseline model from which modifications are made in order to satisfy specific mission objectives.

## **B. ARRAY DESIGN CRITERIA**

Parameters which drive the selection of the array configuration include orbital characteristics, expected satellite service life, reliability, cost, specific power (Watts/kg) and power density (Watts/m<sup>2</sup>).

Orbital characteristics affect both the performance capability and eventual performance degradation of the solar cell array. The power output capability of a solar cell array is a function of the distance from the sun and the angular relationship between the sunline and the solar cell array. [Ref. 1:p. 2.6-1]

The distance from the sun is measured in astronomical units ( $1 \text{ AU} = 1.496 \times 10^{11} \text{ m}$ ) which is the mean sun-earth distance. The total solar power normally incident on a unit area at one AU is defined as the solar constant and is approximately equal to  $1.4 \text{ kW/m}^2$ . This intensity decreases as the distance from the sun increases. However lower solar intensity can have a beneficial effect. About 80 to 90 percent of the energy that falls onto a array goes to heating the array while only 10 to 20 percent is converted by the array into electrical energy. As a result, the solar cell operating temperature decreases thus enhancing solar cell efficiency. Figure 3-3 plots operating temperature variation as a function of solar distance.

Most solar cells are effectively optimized to operate at one solar constant and  $30^\circ\text{C}$ . The output voltage of silicon solar cells decreases with increasing temperature at a rate of approximately  $2 \text{ to } 2.5 \text{ mV } / ^\circ\text{C}$ , while the cell output current increases slightly at a rate of less than  $0.1 \text{ percent } / ^\circ\text{C}$ . Near room temperature, power output decreases with increasing temperature at a rate of approximately  $0.4 \text{ to } 0.6 \text{ percent } / ^\circ\text{C}$ . At approximately  $300^\circ\text{C}$  the energy conversion efficiency of silicon solar cells becomes zero. Figure 3-4 plots the I-V characteristic for a  $10 \text{ ohm-cm}$  silicon cell at operating temperatures ranging from  $30^\circ\text{C}$  to  $150^\circ\text{C}$ .

At certain points in a satellite's orbit, objects such as the moon, earth, planets or other satellites will block the sun. Eclipses disrupt array power output and cause large temperature fluctuations. The most severe environment stresses result from repeated temperature cycling. The number of eclipses experienced over the life span of a satellite depends mainly on the orbit altitude and eccentricity, being

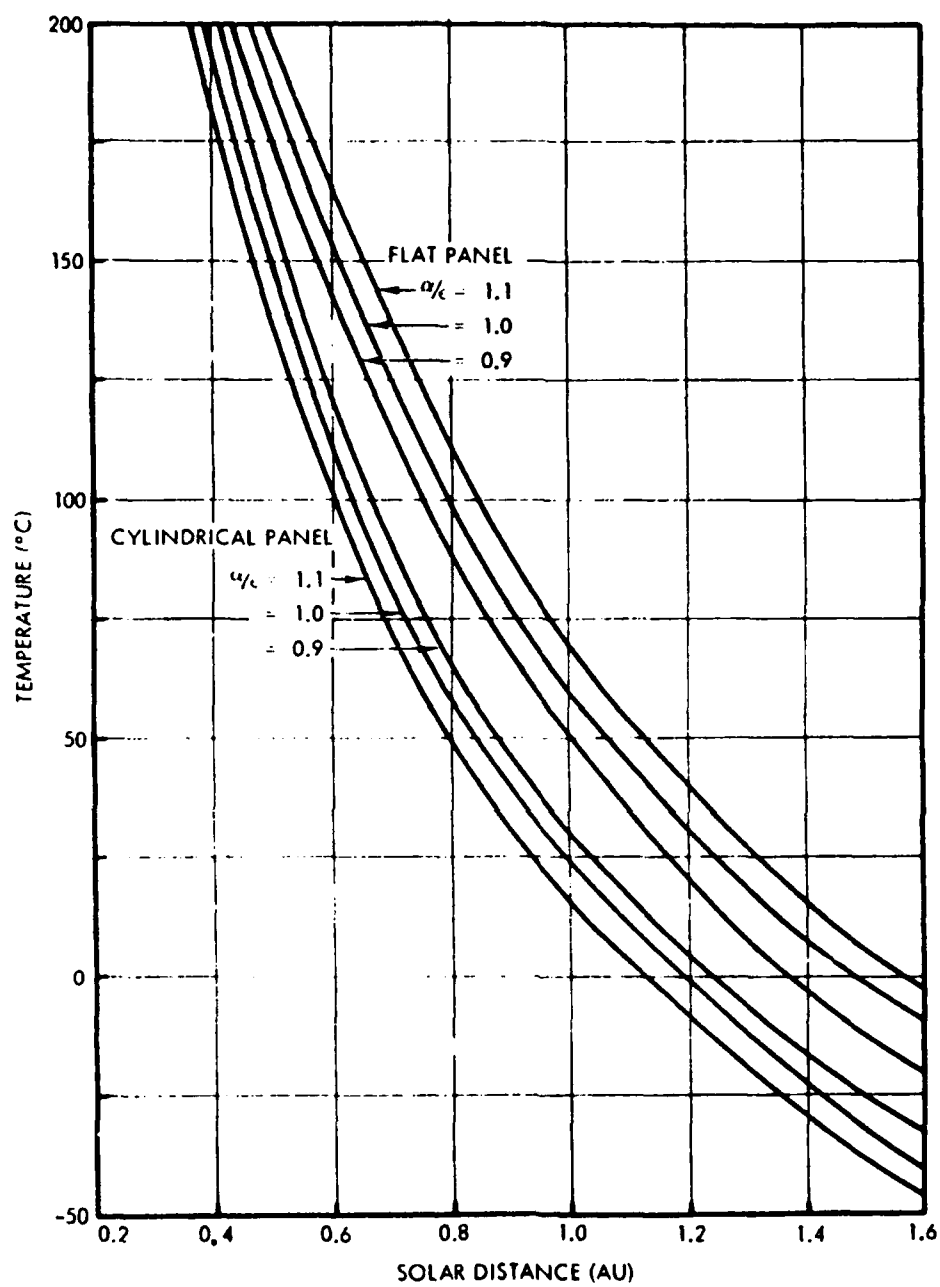
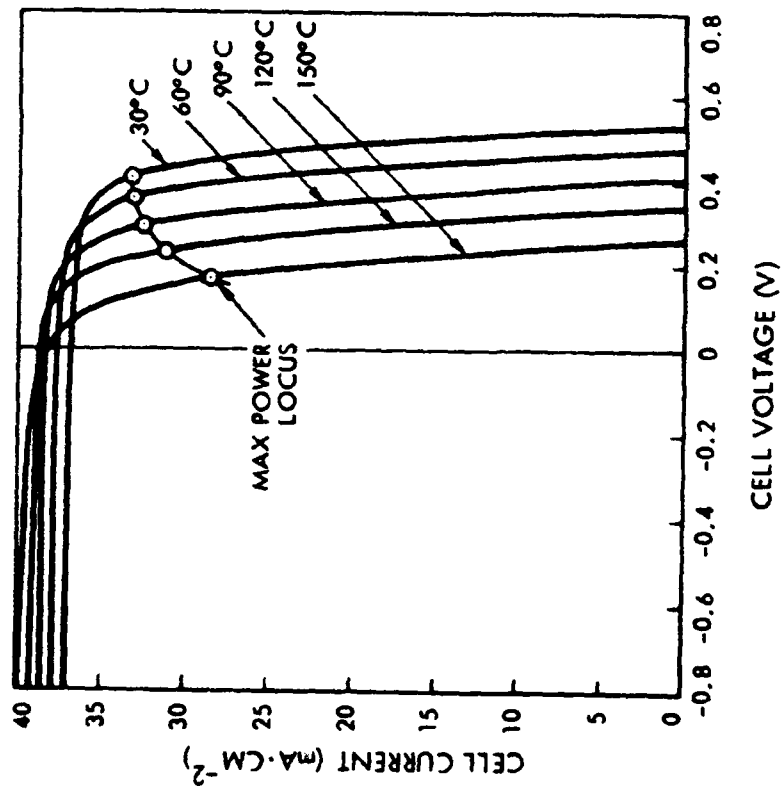
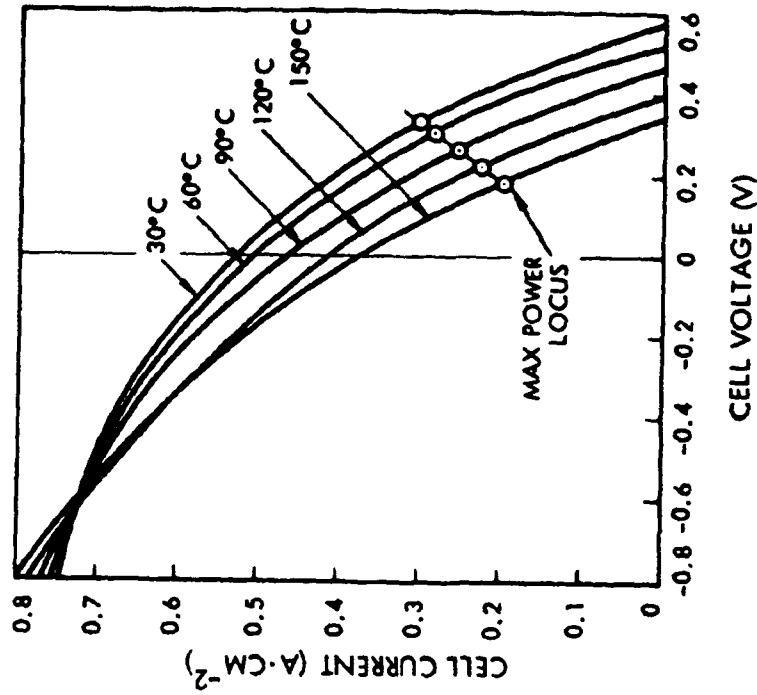


FIGURE 3-3. Operating Temperature Variation. [Ref. 1:p. 8.5-3]





(a) AT ONE SOLAR CONSTANT INTENSITY



(b) AT 20 SOLAR CONSTANT INTENSITY

FIGURE 3-4. Silicone Cell I-V Characteristic Curve [Ref. 1:p. 3.5- 2]

highest for circular orbits at low altitudes. Table 3-1 lists the temperature cycling design requirements for solar arrays.

In addition to temperature cycling, solar performance is degraded by the cumulative damage done by charged particle irradiation. Design life becomes an important criterion for satellites whose orbits will encounter heavy charged particle exposure or severe thermal cycling. The following is a guideline for design life limitations which can be achieved with high confidence.

- Geosynchronous orbit - 10+ years  
( 35,794 km typical)
- Mid altitude orbit - 7 years  
( 10,371 km typical)
- Low earth orbit - 2 years  
(926 km typical)

Extra consideration must be given to solar flares whose occurrence is related to sun spot activity. Sun spots apparently operate on an eleven year cycle. Within the cycle is a seven year period of intense activity or "solar maximum". Most of the solar flare protons that damage solar cells occur in one (or a few) abnormally large flares that seem to occur during a time span of three to four years centered around the middle of the solar maximum activity. [Ref. 1:p. 2.5-3]

There are numerous other attributes that will come to influence the design process. Design margins are tight and system integration is of paramount importance. The mission objectives and the emphasis on reliability, performance and economy will dictate the amount of robustness that can be engineered into the design. There are always time constraints to consider. It is costly to over design. However most designs tend to be conservative for once the satellite is

**TABLE 3-1. TEMPERATURE CYCLING DESIGN REQUIREMENTS**

<b>Orbital Altitude (km)</b>	<b>Orbital Period (hrs)</b>	<b>Number of Cycles per Year</b>	<b>Eclipse Time (hrs)</b>
480	1.57	5580	0.57
926	1.72	5074	0.57
1500	1.93	4526	0.58
10,371	6.0	1460	0.75
35,786	24	365	1.20
107,359	106.0	84	1.89

launched it becomes almost impossible to be able to compensate for unanticipated deficiencies.

### **C. Array Sizing Calculations**

The above considerations will lead to an initial selection of spacecraft / array configuration. Power output requirements determines the size of the array that is needed and thus also determines whether body mounted panels will suffice or if deployable panels are necessary. Then solar cell type , coverglass and substrate are selected. Economic constraints usually control this decision.

#### **1. Maximum Power Output (EOL)**

Solar cell performance degrades with time in orbit. The solar array degradation factor  $F_{RAD}$  are given as the ratio of the cell maximum power output at end of life (EOL) with 1 MeV fluence to the beginning of life (BOL) zero fluence values. Some overdesign is required so that the solar array is able to provide the necessary power output at EOL. The minimum number of solar cells,  $N$ , that is required is found from

$$N = \frac{P_A}{P_C} \quad (3-1)$$

where

$P_A$  = required power output

$P_C$  = degraded power output of a single solar cell.

$P_C$  , the glassed maximum single cell power output at EOL is found from

$$P_C = P_o \times S' \times F_{RAD} \times F_{Top} \times F_M \times F_{SH} \times F_{BD} \times F_{CONF} \quad (3-2)$$

where

$P_o$  = initial, unglased and undegraded solar cell  
output at normal incidence at one solar constant  
AMO intensity and at a reference  
temperature (25°C or 28°C)

$S'$  = effective solar intensity to include the effects  
of cover transmission degradation, solar distance  
and non normal incidence.

$F_{RAD}$  = solar cell degradation factor

$F_{Top}$  = operating temperature degradation factor defined by  
ratio of maximum power output at the operating  
temperature to maximum power at a reference  
temperature.

$F_M$  = miscellaneous assembly and degradation factors

$F_{SH}$  = shadowing factor

$F_{BD}$  = blocking diode and wiring loss factor. [Ref. 1:p. 8.6-1]

Knowing the mass and area /volume of a single substrate and solar cell unit, the volume and weight of the solar array can be found (multiply by N). Specific power (W/kg) and power density (W/m<sup>2</sup>) are figures of merit which can be used to compare the structural efficiency of the substrate design .

## 2. Voltage Level (EOL)

Power output and performance requirements of expected loads are combined and a power budget and load profile are developed. Calculations are

made to ensure that the solar cells are electrically configured to provide specified voltage and current levels. Enough solar cells must be connected in series to provide the bus voltage. This takes into account any voltage drops across blocking diodes and wiring. The required number of cells in series,  $N_s$ , is found from

$$N_s = \frac{V_B + V_D + V_w}{V_{mp}} \quad (3-3)$$

where

$V_B$  = spacecraft bus voltage

$V_D$  = array blocking diode forward voltage drop

$V_w$  = total wiring voltage drop between the solar cells and the load or battery in both the hot and return lines

$V_{mp}$  = solar cell end of mission (or other mission critical event) degraded output voltage at the cell's maximum power point and under operating temperature and intensity. [Ref. 1:p. 8.7-1]

### 3. Load Current

Enough solar cell strings must be connected in parallel to provide the required load current. The required number of parallel strings,  $N_p$  is found from

$$N_p = \frac{I_L}{I_{mpav}} \quad (3-4)$$

where

$I_L$  = required load current

$I_{mpav}$  = average maximum power point current output of all  $N_p$  strings that are connected in parallel after glassing

and degradation, at the operating temperature,  $T_{Op}$ ,  
and under reduced illumination conditions due to cover  
darkening and non normal incidence. [Ref. 1:p. 8.7-1]

#### 4. Reverse Bias Solar Cells

In the normal power generating mode of an illuminated solar cell, the output voltage measured from the p-contact to the n-contact is positive. The cell is forward biased.

When an external source forces additional current through a solar cell in the same direction as the cell's photo-induced current, the voltage across the cell decreases. If the sum of the photo-induced current and the current from the external source is greater than the cell's short circuit current, then the voltage measured from the p-contact to the n-contact will be negative and the cell is referred to as reverse biased. When reverse biased, the current through a solar cell is referred to as the reverse current, although it is the voltage that is reversed from the normal, not the direction of the current. Reverse biased solar cells dissipate power as heat rather than generate power.[Ref. 8:p. 1]

If one or more cells in an electrical string become shadowed, the shadowed cells can become reversed biased. The voltage across a shadowed cell can be found from

$$V_{SH} = V_{STR} - V_{IC} \quad \text{with } V_{IC} \leq V_{OCI} \quad (3-5)$$

where

$V_{SH}$  = voltage across the shadowed cell

$V_{STR}$  = voltage across entire string

$V_{IC}$  = voltage across illuminated circuit

$V_{OCI}$  = open circuit voltage of the illuminated circuit.

[Ref. 8:p. 2]

The degree to which a shadowed cell in an array can become reverse biased depends on

- the open circuit voltage of the illuminated cells in the string
- the operating bus voltage level
- the reverse current characteristic of the shadowed cell

Space power systems having a large number of solar cells in series need to minimize the difference between bus operating voltage and open circuit voltage.[Ref. 8:p. 4]

The above equations are a simplified version of the actual calculations that are performed as part of the array sizing process. This thesis presents only a brief overview of the factors involved in solar cell design and electrical performance prediction. A more in-depth treatment can be found in Reference 1. Figure 3-5 summarizes the parameters that affect the electrical parameters of a solar cell. Variation of one parameter impacts more than just one area of design and may cause other input parameters to change as well.



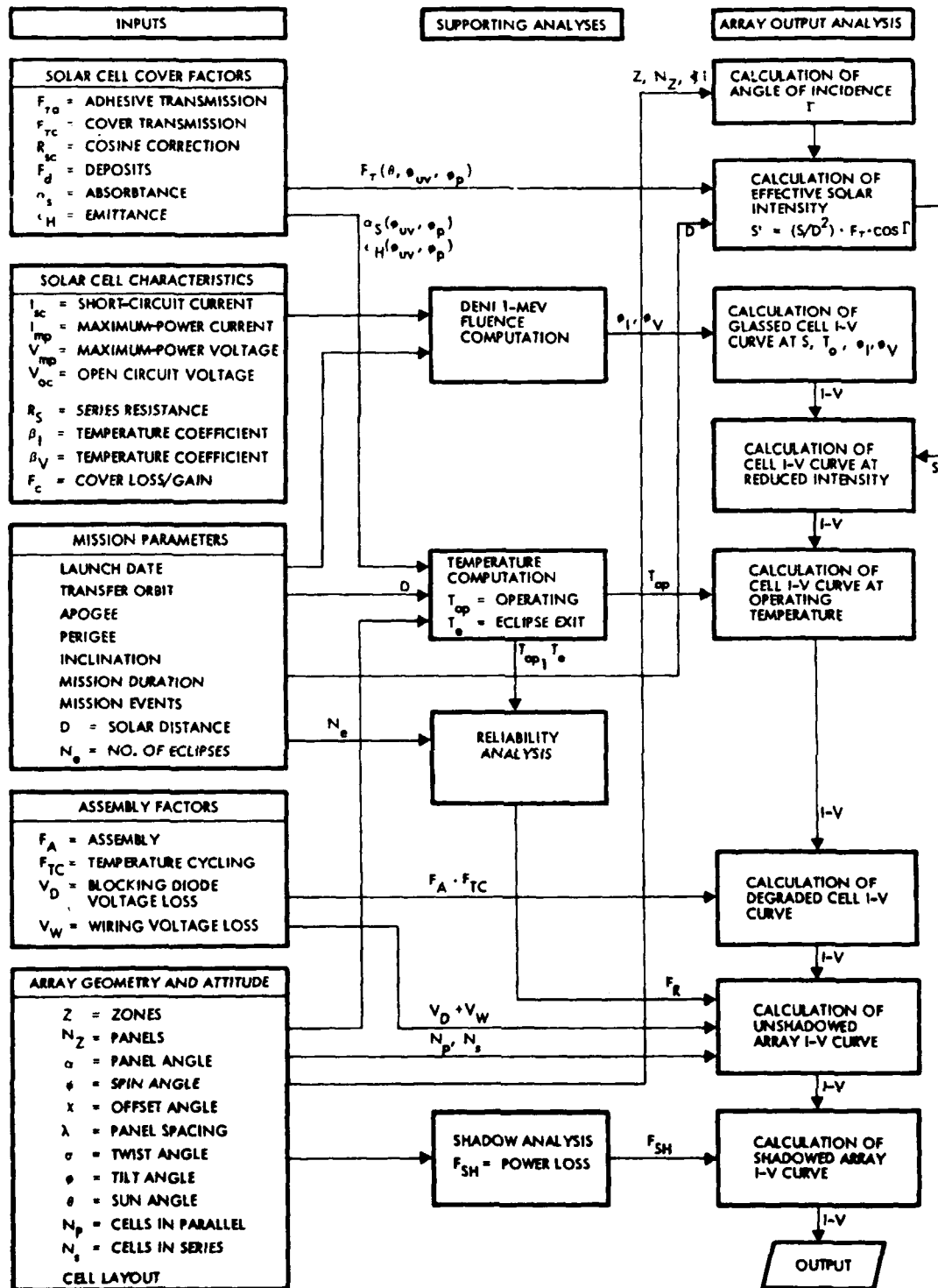


Figure 3-5 - Solar Cell Electrical Performance Prediction Parameters  
[Ref. 1:p. 9.4-2]

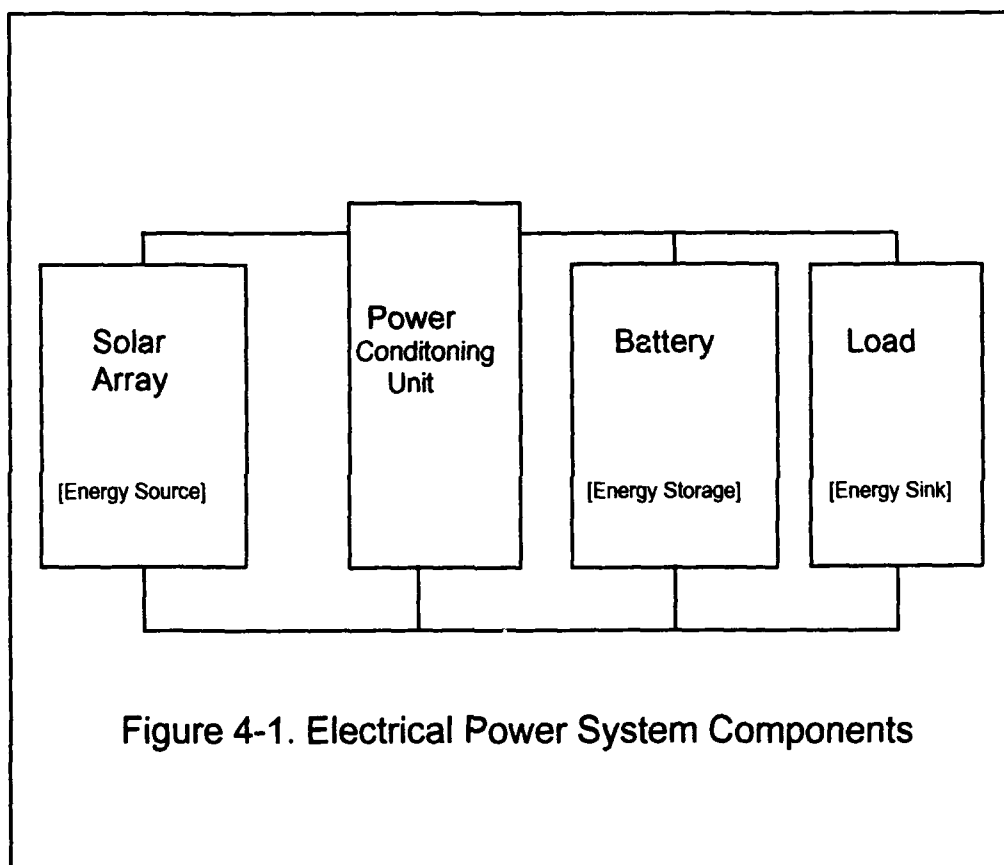
## **IV. SPACE ELECTRICAL POWER SYSTEM**

### **A. POWER SYSTEM COMPONENTS**

The design of an electrical power system typically begins with identifying loads and specifying power requirements. The power output and power quality demanded by the load define the specifications that the electrical system must meet. Figure 4-1 shows the typical components which comprise a space electrical power system. Solar arrays generate power which is regulated and distributed to the load. This power is dependent on the available illumination and thus is sporadic falling to zero during eclipse periods. Batteries are energy storage reservoirs which stabilize power output, providing power during peak load demands and eclipse periods. They must be recharged during times of low load demand when the solar array has excess power.

#### **1. Power Conditioning Unit**

The two basic types of power conditioning units are Direct Energy Transfer (DET) (also called shunt system) and Peak Power Tracking (PPT). In a DET system, the solar array is directly connected to the load through a shunt diode. This shunt diode will dissipate excess solar array power not being used by the load or for battery recharge. Bus voltage is unregulated varying between the solar array voltage level during times of illumination and battery voltage level during periods of eclipse or shadowing. More complicated variations of this system exist in which the bus voltage is regulated to maintain a set value and battery charge and discharge power is monitored. [Ref. 10:p. 47]



In contrast, the PPT electronically adjusts the effective load of the solar array for maximum array power. The solar array operating point is adjusted by a pulse width modulated (PWM) switching regulator whose duty cycle is controlled by load demand. This feedback design enables the system to track the maximum power operating point of the array. [Ref. 11:p.1]

The PPT more effectively uses the power generated by the array. This allows the array size to be reduced for a particular mission or the number of flight experiments to be increased. The power operating point for a DET system must be biased below the maximum power point to allow for worst case array variations due to illumination, temperature, radiation, degradation and partial failure. However the DET system has been most commonly used because of its simplicity and relatively low parts count. Note that some power is consumed by the switching circuitry and power processing electronics of the PPT design. In addition, electromagnetic interference (EMI) is generated by the PPT power system electronics which may have adverse effects on other electronic equipment. [Ref. 11:p. 1]

## **2. Battery**

Nickel cadmium batteries have been the mainstay of rechargeable space batteries for the past twenty years. These batteries can deliver energy densities ranging from 7 to 15 Watt-hours/kg depending on the orbit altitude (number of charge/discharge cycles). Nickel cadmium batteries been replaced by nickel hydrogen batteries which typically deliver 20 Watt-hour/kg in low orbit and 40 Watt-hour/kg in geosynchronous orbit. [Ref. 12:p. 4]

Currently in development, sodium sulfur batteries have shown great promise of becoming the next generation, high performance battery for space applications. First generation sodium sulfur batteries have demonstrated power densities of 70 Watt-hour/kg for low cycle lifetimes typical of geosynchronous orbits (1000 cycles). Work has begun on a second generation sodium sulfur battery with a goal of 200 Watt-hour/kg. Anticipated advances in both battery and solar array performance will make future solar array/ battery powered systems with specific power capabilities of 45 W/kg possible as compared to the 7-10 W/kg systems presently available.

The primary purpose of the battery is to provide the needed power during eclipse periods. The battery should be fully charged before each eclipse period. The parameters that affect the battery's ability to be fully charged include the battery temperature and available charge current and voltage from the solar array.

[Ref. 13:p.199]

Typical battery operation is as follows.

The satellite demands power from the battery when the eclipse starts. The battery generates a large amount of heat during its discharge. Even with a well designed heat removal system, the battery temperature is expected to rise rapidly during this discharge. At the end of the eclipse and as soon as the solar array can provide power, the battery is charged to be ready for the next eclipse discharge. The beginning of the battery charge cycle results in a brief period of endothermic operation during which the battery cools rapidly. Battery heaters may be needed to prevent the battery from reaching an undesirably low temperature. As the battery approaches overcharge it becomes exothermic and its temperature increases again.

[Ref. 14:p. 1377]

The following constraints must be met for successful battery operation:

- Maximum temperature must remain below a set value

- to avoid damage to the battery or shortening its life.
- Minimum temperature must not be too low so as to reduce battery efficiency or freeze the battery electrolyte to render it inoperable.
- As the battery nears full charge, its voltage must be lower than the available solar array charge voltage so that the charge can continue.
- The charge current must be sufficiently high so that full charge can be arrived at before the next eclipse.

[Ref. 14:p. 1377]

A battery consists of electrochemical cells connected in series and parallel so as to provide the specified voltage and current. Battery performance is rated in terms of voltage level and current capacity (amp-hr). The required battery bus voltage will determine the number of cells that must be hooked in series. The number of parallel batteries is found from

$$N_1 = \frac{AH_{reqd}}{DOD_{max} * AH_{rated}} \quad (4-1)$$

where

$AH_{reqd}$  = current capacity required by the load

$AH_{rated}$  = rated current capacity of a single battery

$DOD_{max}$  = maximum rated depth of discharge of the battery

and

$$N_2 = \frac{P_{DM}}{V_{AD} * I_M} \quad (4-2)$$

where

$P_{DM}$  = maximum steady state discharge power required by the load  
during eclipse

$V_{AD}$  = the average discharge voltage of the battery

$I_M$  = the maximum discharge current of the battery.

Both equations must be satisfied. The first equation takes into account the required current capacity while the second equation considers the power output requirement. The higher number ( $N_1$  or  $N_2$ ) will determine the number of parallel batteries needed. [Ref. 15:p. 70]

Selection and sizing of the battery impacts not only the electrical system power output and performance but also the mission life duration of the satellite. The battery operating life is sensitive to the regimen it is subjected to. The main factors that define this regimen are temperature, depth of discharge (DOD) and charge/discharge rates. The battery must be sized so that the rated maximum DOD and discharge rate is not exceeded. [Ref. 13:p. 199]

Other battery design issues include providing adequate structural support for the battery during launch and while in orbit. The battery housing must incorporate methods for heat dissipation during battery discharge as well as provide insulation when temperatures fall too low.

### **3. Load Profile**

It is of paramount importance to provide sufficient power for onboard loads to include equipment performing housekeeping functions such as command signaling and power conditioning. The satellite's orbit will define its illumination profile. Thus the amount of solar energy available as a function of time during orbit in space is known. A power budget is formulated, allocating power to loads

at the nominal rated value and for the nominal duration of expected usage. The power that the solar array provides must equal or be greater than the power that is required to operate satellite equipment and to properly manage its battery.

The electrical system must efficiently allocate the available power to the various onboard loads as well as dynamically redistribute power during sudden surges in demand or reduction in supply. When power demand exceeds the available supply, removal of less critical loads may be necessary. Sensitive loads must be protected from transient disturbances.

## **B. SYSTEM INTEGRATION**

Each component of the electrical power system is carefully selected so as to meet performance specifications. This selection process may involve laboratory testing to verify that capacity and life cycling/duration requirements are met. Mathematical models are derived and computer simulations done to predict performance in a space environment. Any previous flight history is analyzed.

Even though each component is individually tested, satisfactory performance of the overall electrical power system is not guaranteed. There are many competing and conflicting system constraints. Each component must interface properly with the system. The operation and interaction of these components can be quite complicated and intricate. Components which operated properly when bench tested in the laboratory may malfunction when connected to the system. Certain equipment may degrade the power quality of the electrical power system generating unwanted harmonics, EMI and transient voltage and current surges.

Subtle changes in any component can have a significant effect on overall system performance. The design process is iterated many times to optimize



performance (trade-off studies) and accommodate any needed changes. Again proven designs are analyzed and the electrical power system is modeled to predict both its dynamic response and its lifetime performance.

### **C. PANSAT ELECTRICAL POWER SYSTEM**

PANSAT, Petite Amateur Navy Satellite, is the Naval Postgraduate School's first endeavor in the design and construction of a space communication satellite. The satellite will provide digital over the horizon communications. The satellite will receive data packets from one site location, store this data packet and later forward this data packet to another site location. This satellite will employ direct sequence spread spectrum modulation techniques. This project is directed by the Space System Academic Group at the Naval Postgraduate School and involves faculty and students from a broad range of disciplines.

The satellite is a 26 sided polyhedron (rhombicuboctahedron) having 18 square and 8 triangular panels. The sides of both the square and triangular panels measure approximately 18.4 cm. Its diameter is approximately 19 inches. It will not weigh more than 68 kg (150 lb).

Solar panels will be mounted on 17 of the 18 square panels. The remaining square panel will be used as a baseplate for integration with the launch vehicle. The satellite will be injected into a low earth orbit as a Get Away Special (GAS) payload which will be launched from a canister in the space shuttle cargo bay. Communication antennas will be mounted on the triangular panels.

The solar array size is limited to approximately 5755 cm<sup>2</sup>, the combined area of the 17 square panels. Due to cost constraints and for simplicity of design, deployable panels will not be used. Once in orbit, the satellite will tumble freely

in space. The effective solar array area was calculated to be 1259 cm<sup>2</sup>. [Ref. 16:p. 3] This calculation was based on the assumption that the satellite's spin axis relative to the sun was random so that each panel would receive equal exposure while tumbling. Note that the lowest effective solar array area occurs when the base panel is normal to the sun vector. The electrical power system (EPS) would not supply the required power for this condition should it become the predominant tumbling mode. [Ref. 17:p. 13]

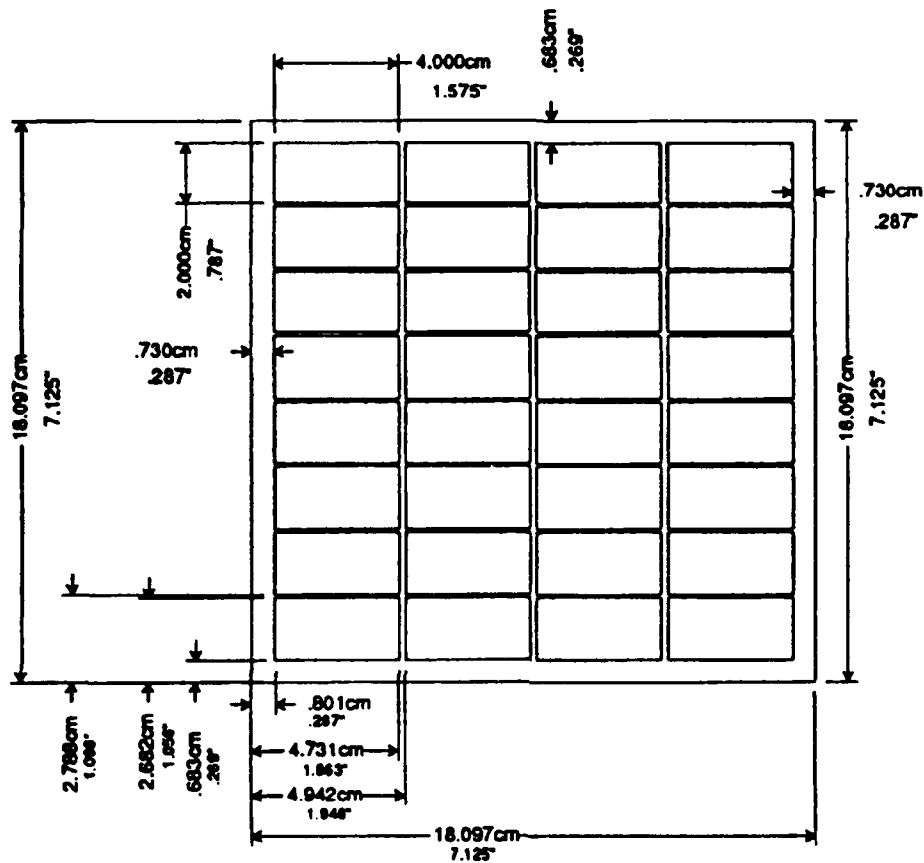
Each square panel has 32 solar cells connected in series to form an electrical string. The 17 electrical strings are connect in parallel through a blocking diode to the bus. Solar cell panel dimensions are shown in Figure 4-2. The EPS has two batteries each of sufficient capacity to meet mission requirements. Battery charging is accomplished through processor controlled pulse width modulation of the array output. DC to DC convertors are used to provide power conditioning for specific equipment.

A preliminary design for the PANSAT EPS was done in a thesis by M. Noble. (See Reference 17.) The design calculations were performed assuming that silicon solar cells were to be used. Present designs are also based on silicon solar cells, however higher conversion efficiency is specified. The solar array configuration is summarized in Table 4-1.

There have been other changes to the preliminary design. Components such as the battery have been upgraded. Requirements such as EOL power output have increased. PANSAT EPS began as a direct energy transfer design with a 12 volt unregulated bus. It is being redesigned to a peak power tracking system. The voltage level in each string and the temperature of each panel is to be monitored. These are listed in Table 4-2.

Figure 4-3 shows a schematic of PANSAT's power distribution system. The EPS is still in the early design phase. Many parameters are not yet known since PANSAT's exact orbit altitude and inclination have not been defined. Design of the onboard communication equipment is being done concurrently. Dynamic load behavior has not yet been analyzed. Table 4-3 is an estimated power budget.

The PANSAT EPS is designed to meet expected EOL conditions and not for combinations of all worst case conditions. Enough parameters have not yet been defined to permit system simulation and performance prediction.



Solar cell array panel made up of (32) 2 cm x 4 cm cells, with packing efficiency of 95%.

Allows approximately 1/4 in for panel mounting.

FIGURE 4-2. PANSAT Solar Array Panel Dimensions [Ref. 18]

## POWER DISTRIBUTION

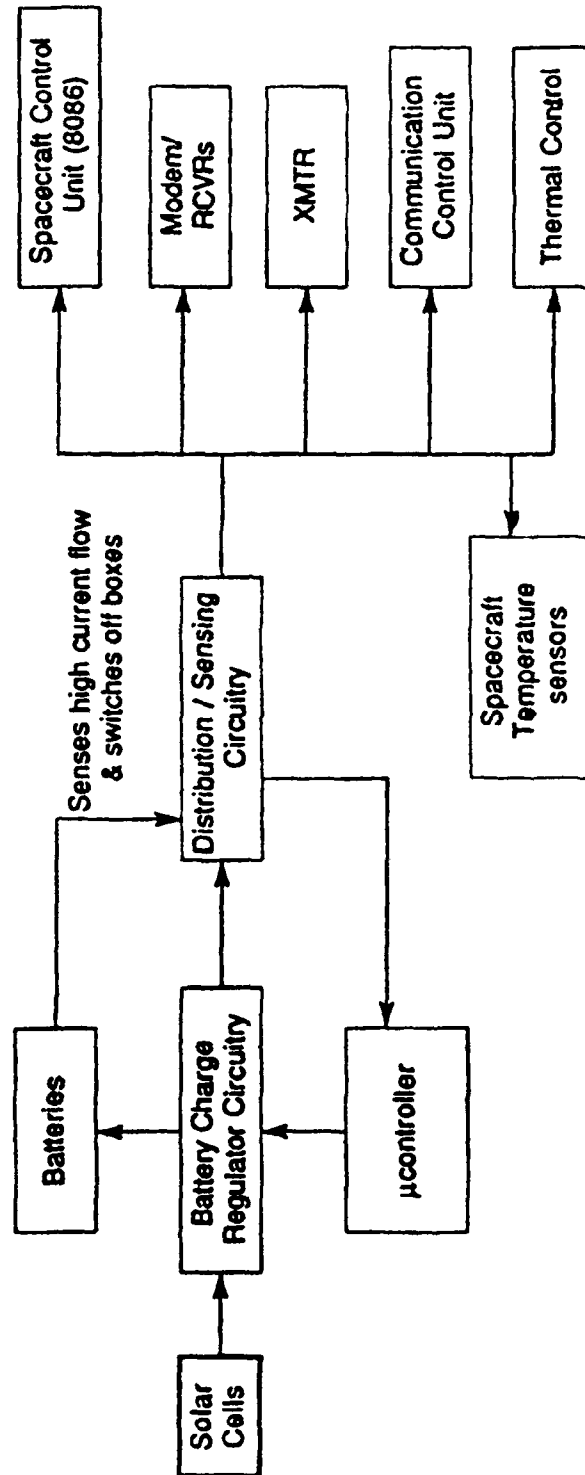


FIGURE 4-3. PANSAT Power Distribution System [Ref. 19]

TABLE 4-1. PANSAT SOLAR ARRAY CONFIGURATION

<p>Summary Description: 17 identical body mounted panels, each panel measuring 18.1 cm x 18.1 cm, each panel comprises an electrical string of 32 single cell in series, 17 electrical strings connected in parallel. Blocking diodes will isolate each string from voltage bus, these diodes will not be physically mounted on the panels, but will be contained in the Solar Array Junction Box inside the spacecraft.</p>		
Description	Preliminary Design [M. Noble Thesis]	May 1992 Specifications
Cell type	K6700 silicone BSR, BSF, N/P shallow diffused, BSR, BSF, DAR coating	not specified - silicone, GaAs, InP N/P shallow diffused, BSR, BSF, DAR coating
Cell size	2 cm x 4 cm x 0.01 cm	2 cm x 4 cm x 0.02 cm
Resistivity	10 ohm-cm	10 ohm-cm
Conversion efficiency at 28°C	14.3%	14.5%
Coverglass	6 mils CMX	30 mils Corning Glass 7940 fused silica or NPS approved equivalent  Ultra - Violet Transmission 1% for 0.250-0.320 $\mu$ m wavelength 50% at 0.350 $\mu$ m $\pm$ 0.015 $\mu$ m 87% at 0.450 -1.00 $\mu$ m minimum 92% minimum average at 0.50-1.00 $\mu$ m
Coverglass to Cell adhesive	Dow Corning 93-500 Silicone	Dow Corning 93-500 Silicone
Cell - Substrate Insulation	0.2 mm Kapton	unspecified - must provide 100 mega ohms of resistance
Cell to Insulation adhesive	RTV - 118	McGhan Nusil CV2568 silicone, Dow Corning 93-500 or NPS approved equivalent
Substrate	2014-T6 sheet aluminum	6061-T6 aluminum

TABLE 4-2. PANSAT SOLAR ARRAY REQUIREMENTS

Requirement	Preliminary Design [M. Noble Thesis]	May 1992 Specification
Nominal Orbit	480 Km. 0°. circular	800Km. 0°. circular
Lifetime	2 years	2 years
Temperature Range	-160°C to 100°C	-65°C to 140°C
Minimum Output Power (EOL)	17.6 W	24.5 W
Average Power (BOL)	18.3 W	unspecified
Minimum Panel Voltage (EOL)	13.3 V	12.0 V
Single Cell Characteristics:		
$V_{OC}$	595 mV	600 mV
$I_{SC}$	43.25 mA/cm <sup>2</sup>	42.5 mA/cm <sup>2</sup>
$P_{MP}$	19.53 mW/cm <sup>2</sup>	19.8 mW/cm <sup>2</sup>
Battery		
Type	Gates lead acid (X-Cell)	NiCd or NiH
Capacity	60 Wh	48 Wh
Fully charged voltage	12.6 V	unspecified
Power Conditioning	DET - 12V unregulated bus	PPT

**TABLE 4-3 PANSAT POWER BUDGET**

<b>Satellite Component</b>	<b>Peak Power (W)</b>	<b>Standby Power (W)</b>	<b>Duty Cycle (% / orbit)</b>
<b>Spacecraft Control Unit (CPU)</b>	2.5	1.0	100%
<b>Communications Control Unit (CPU)</b>	1.0	1.0	100%
<b>Transmitter</b>	11.0	1.0	30%
<b>Receiver</b>	3.0	1.5	100%
<b>Power Control Unit (CPU)</b>	1.0	1.0	100%
<b>Battery</b>	6.0	1.0	50%
<b>Total</b>	<b>24.5</b>	<b>6.5</b>	



## V. SUN SENSORS

Solar cells pass no (or negligible) current in the dark. In sunlight it passes  $I_{SC}$  which is proportional to the illumination intensity and incidence angle of the incoming rays. This behavior makes solar cells an ideal sensor for the sun. Solar cells operating in the sensor mode are called photodiodes. Photodiodes are suitable in low noise, low frequency applications.

Sun sensors are the most widely used sensor types in spacecraft. They determine the relative angle between the spacecraft and the sun. This information can then be used for attitude control, safemode operation (provide indication of when to activate and deactivate light sensitive equipment) and solar array positioning.

The sun sensor owes its versatility to several factors. Unlike the earth, the angular radius of the sun is nearly orbit independent and sufficiently small (0.267 degrees at one AU) that for most applications a point source approximation is valid. This simplifies both sensor design and attitude determination algorithms. The sun is sufficiently bright to permit the use of simple, reliable equipment without discriminating among sources and with minimal power requirements. [Ref. 20:p. 155]

Sun sensors are usually not the only sensor used onboard a space vehicle for there may be times during the orbit when the sun is blocked. There are basically two types of sun sensors available commercially -- analog and digital.

### A. ANALOG SUN SENSORS

Analog sun sensors exploit the solar cell  $I_{SC} \cos \theta$  dependence, where  $\theta$  is the angle of the incoming ray measured from a vector normal to the face of the solar cell. Analog sun sensors are also called cosine detectors.

A common configuration connects two photodiodes positioned at different angles such that the current output of the cells oppose each other. If the sun shines more on one cell than the other, current will flow in a certain direction. If the sun is precisely between the cells, both will receive the same illumination and there will be no current flow. This is illustrated in Figure 5-1. [Ref. 20:p. 158] This configuration will give the sun's orientation with respect to one axis. Four photodiodes can be positioned in quadrature to provide two axis coverage.

Another analog sensor configuration uses a bar or mask to shadow a portion of one or more photodiodes. The photodiodes are arranged such that different angles will shadow one photodiode more than another.  $I_{SC}$  generated will depend on how much area of the photodiode is shadowed and thus through geometry the relative angle between the sun and the photodiode can be determined. Different configurations can yield a one axis sensor (Figure 5-2) or a two axis sensor (Figure 5-3) with varying field of views and resolution.

## **B. DIGITAL SUN SENSORS**

Digital sun sensors encode the sun angle into a binary code. Light passes through a slit and forms an image on columns of solar cells. (See Figure 5-4.) The image formed depends on the angle of incidence of the ray coming through the slit. A two axis digital sun sensor is shown in Figure 5-5.

Various sun sensors manufactured by ADCOLE Corporation are listed in Table 5-1. Digital sun sensors accurate to  $0.017^\circ$  are available. Digital systems however consume more power (up to 17W) and generally weigh close to two pounds. Analog systems are very light weight (less than 0.2 pounds) and in most cases require no input power.

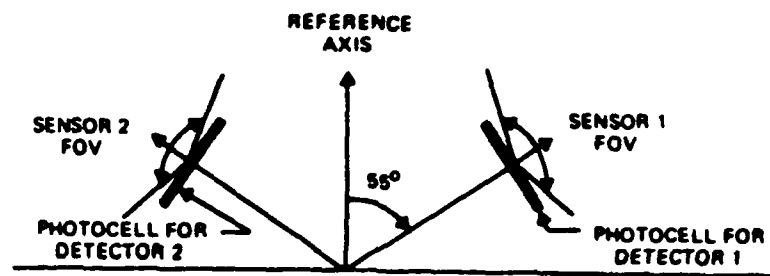


FIGURE 5-1a. Analog Sun Sensor - One Axis [Ref. 20:p.158]

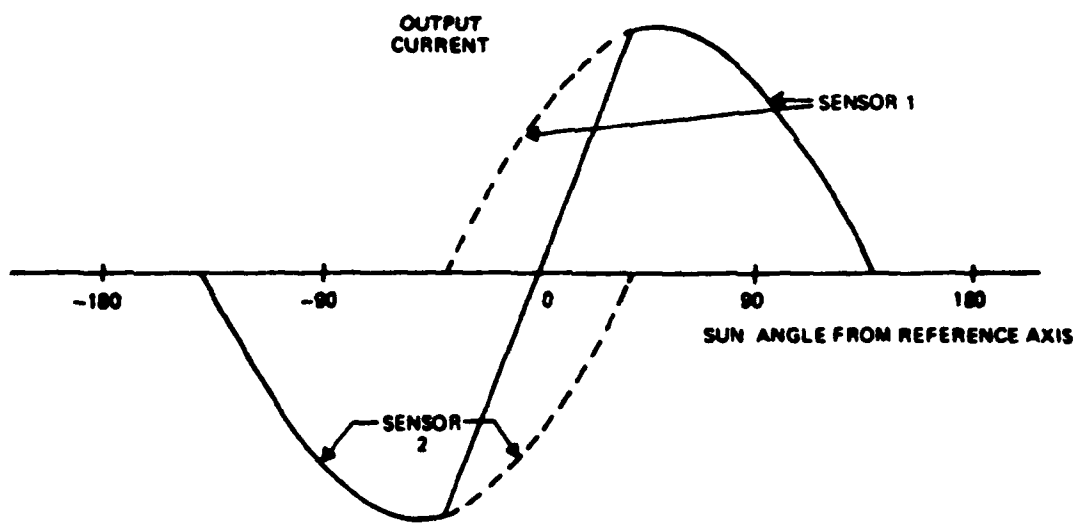


FIGURE 5-1b. Summed Output of Analog Sun Sensor Photocells [Ref. 20:p. 158]

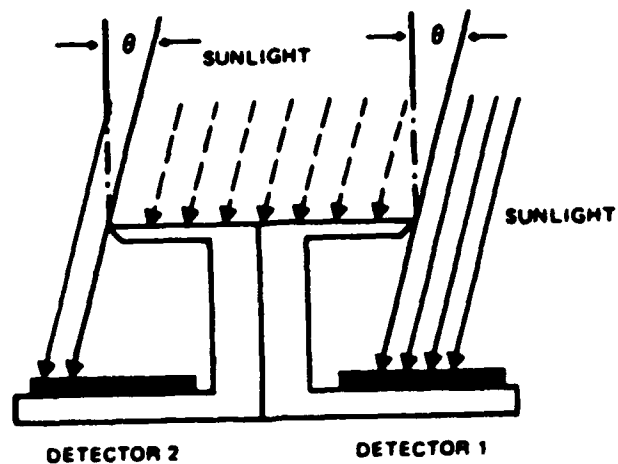
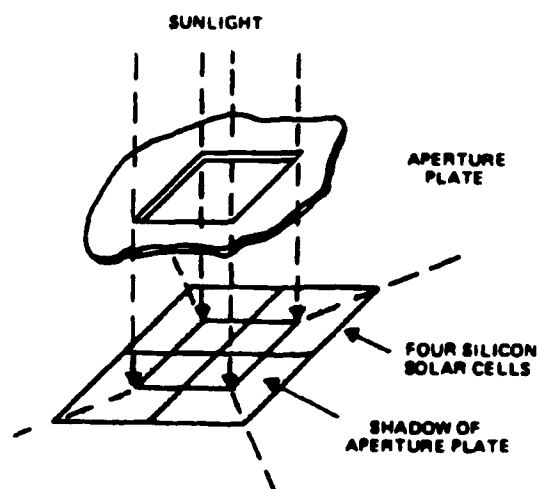


FIGURE 5-3. One Axis Analog Mask Detector [Ref. 20:p. 158]



**Two-Axis Mask Sun Detector** The sunline is normal to the aperture plate if the output of all four solar cells is equal.

FIGURE 5-3. Two Axis Analog Mask Sun Sensor [Ref. 20:p. 159]

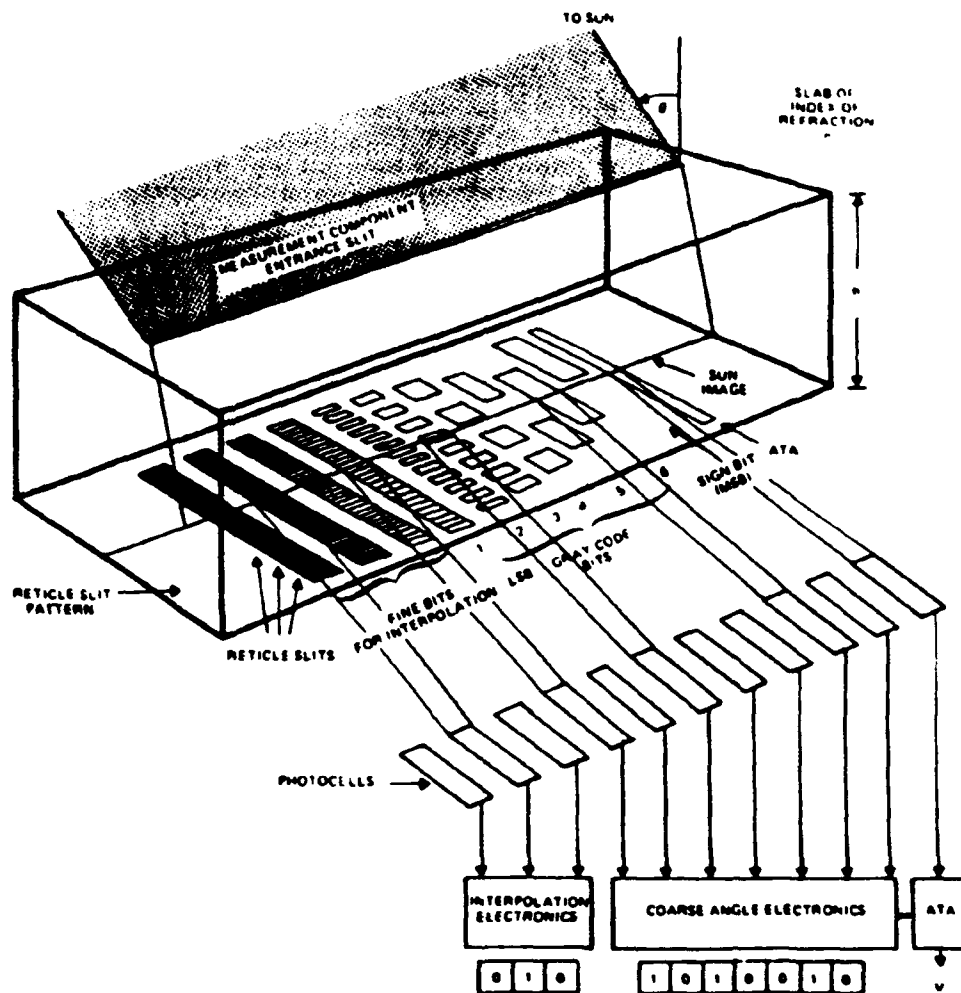


FIGURE 5-4. One Axis Digital Sun Sensor [Ref. 20:p. 163]

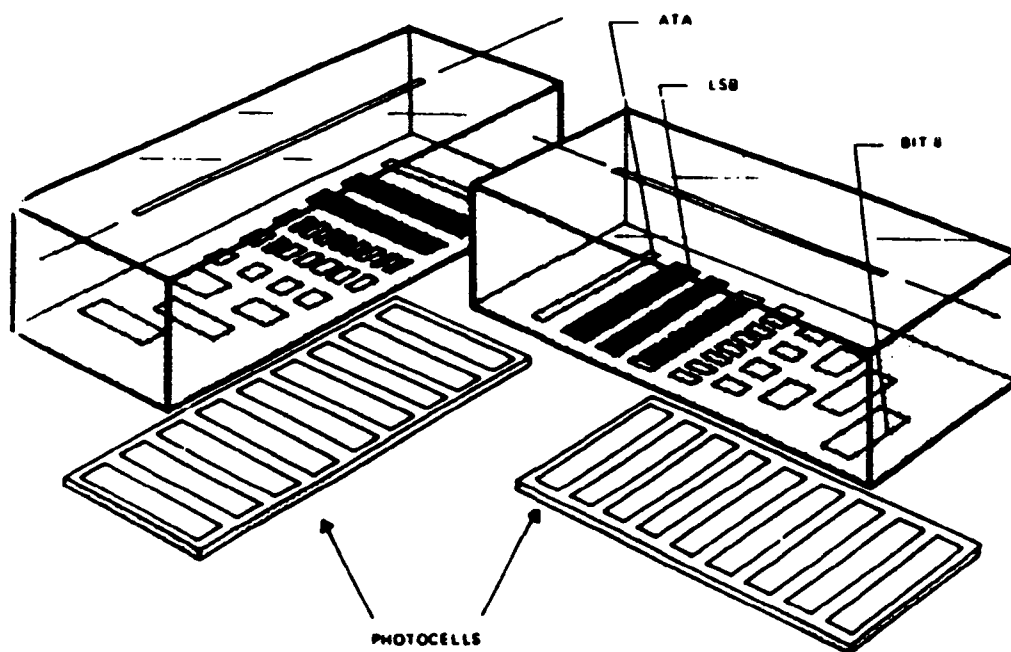


FIGURE 5-5. Two Axis Digital Sun Sensor [Ref. 20:p. 166]

Representative Sun Sensors Produced by Adcole Corporation. (Data Courtesy Adcole.)

SENSOR	ADCOLE MODEL NUMBER	FIELD OF VIEW	MAXIMUM NUMBER OF MEASUREMENTS PER HOUR <sup>2</sup>	LEAST SIGNIFICANT BIT	ACCURACY <sup>4</sup>	TRANSFER FUNCTIONS	OUTPUT <sup>10</sup>	ELECTRONICS		SENSOR	WEIGHT (gm)		INPUT POWER	SUNSHINE FLOW
								ELECTRONICS	SENSOR		ELECTRONICS	SENSOR		
DIGITAL SENSOR FOR SPOONING VEHICLES	11882	180°	1	1 <sup>0</sup>	0.00°	180	9-BIT SERIAL GRAY CODE	84 ± 81 × 80	51 × 51 × 31	448	141	-24.5 watt 12 mm	AT-2, 3, 4, 5, 6, 8, 9, 10, 11	
	15701	90° <sup>1</sup>	1	0.00°	0.1°	171	9-BIT SERIAL BINARY CODE	102 ± 80 × 80	33 × 33 × 33	340	100	-1.5 watt 80 mm -0.0 watt 4 mm -0.0 watt 4 mm	AEPOLE-1 AEPOLE-2	
		180° <sup>1</sup>	1	1 <sup>0</sup>	0.0°	180	9-BIT SERIAL GRAY CODE		48 × 43 × 20		100			
		60° <sup>1</sup>	2	0.20°	0.1°	180	9-BIT SERIAL GRAY CODE		68 × 38 × 25		100	-20 watt 800 mm	CTS	
TWO-AXIS DIGITAL SENSORS	18272	120° × 120°	5	1 <sup>0</sup> <sup>2</sup>	0.0°	180	7-BIT/AXIS SERIAL GRAY CODE	153 ± 114 × 84	84 × 41 × 18	1043	73		AT-4	
	15400	120° × 120°	1	1 <sup>0</sup> <sup>2</sup>	0.0°	180	7-BIT/AXIS PARALLEL GRAY CODE	76 × 76 × 51	84 × 41 × 18	308	82	-15 watt 10.5 mm	AT-4	
	17115	120° × 120°	3	1 <sup>0</sup> <sup>2</sup>	0.0°	180	7-BIT/AXIS PARALLEL GRAY CODE	108 ± 114 × 84	84 × 41 × 18	987	113	5.0 to 3.0 watt 12 mm	AT-4, GEOM-3, SAS-3, 4, 5, 6, 7	
	16704	120° × 120°	5	0.0° <sup>3</sup>	0.20°	180	8-BIT/AXIS PARALLEL 3-BIT/IDENTITY GRAY CODE	80 ± 114 × 31	81 × 81 × 20	200	200	-12 to 30 watt 8 mm -12 to 30 watt 2 mm	AEPOLE-1 <sup>11</sup>	
	17022	60° × 60°	4	0.120° <sup>3</sup>	0.1°	180	9-BIT/AXIS SERIAL GRAY CODE	107 ± 114 × 80	97 × 31 × 23	1148	277	-24.5 watt 500 mm	MINIBUS-4	
	15301	60° × 60°	1	0.000° <sup>3</sup>	0.01°	180	10-BIT/AXIS PARALLEL BINARY CODE	108 ± 114 × 84	97 × 104 × 25	1361	372	-20 watt 61.5 mm	QAO-3	
	18800	60° × 60°	2	0.000° <sup>3</sup>	0.01°	180	15-BIT/AXIS SERIAL GRAY AND BINARY CODE	200 ± 107 × 30	84 × 110 × 25	486	341	-20 watt 1.8 m	144 SEASAT <sup>11</sup>	
TWO-AXIS ANALOG SYSTEM	17297	30° CONE	N/A	N/A	1 AT NULL	1 <sup>0</sup> LINEAR	14 mm	N/A	84 × 30 × 32	NONE	56	NONE	QAO-3, 3, 4, 5, 6, 7	
	18304	FULL HEMISPHERE	1	N/A	2 AT NULL	1.20° LINEAR	10.1 mm PEAK	N/A	48 × 48 × 33	NONE	82	NONE	QAO-3, 3, 4, 5, 6, 7	
SINGLE-AXIS ANALOG SYSTEM	17470	60° × 60°	1	N/A	5 AT NULL	1 <sup>0</sup> LINEAR	0-5° 2.5 AT NULL	88 × 51 × 28		110		-15 to 8 watt 100 mm	CTS	
COSINE-LAW ANALOG	11888	180° CONE	N/A	N/A	2.0°	COSINE OF ANGLE OF INCIDENCE	0.1 mm PEAK	N/A	23.6 mm × 10	NONE	4.6	NONE	QAO-3, 3, 4, 5, 6, 7	

<sup>1</sup>THE FIELD OF VIEW IS SHOWN AS AN OUTPUT PULSE IS PROVIDED WHEN THE PAN CROSSES THE SUN AND THE DIGITAL SUN ANGLE IS READ AT THIS TIME AND STORED. THE SENSOR SHOULD BE MOUNTED SO THAT THE PLANE OF THE PAN IS PARALLEL TO THE SPIN AXIS.

<sup>2</sup>SUPPORTED BY ELECTRONICS

<sup>3</sup>THE LEAST SIGNIFICANT BIT SIZE IS AN AVERAGE OF THE ONE AXIS STEP SIZES OVER THE FIELD OF VIEW.

<sup>4</sup>FOR A DIGITAL SENSOR, THE ERROR IS DEFINED AS THE ABSOLUTE VALUE OF THE DIFFERENCE BETWEEN THE SUN ANGLE CALCULATED FROM THE TRANSFER FUNCTION AND THE ASSUMED ANGLE AT A STEP.

<sup>5</sup>SEE SECTION 7.1 AND FIG. 7.8 FOR A DERIVATION OF TRANSFER FUNCTIONS AND SENSOR ANGLES.

<sup>11</sup>PROPOSED

TABLE 5-1. AD COLE Sun Sensor Models [Ref. 20:p. 165]

### **C. PANSAT SUN SENSOR IMPLEMENTATION**

While tumbling freely in space, PANSAT's body mounted solar panels will receive exposure to sunlight at different angles and will generate varying levels of power. It is reasonable to assume that there is a way to correlate the power generated in each panel with the panel's orientation towards the sun.

PANSAT will have solar panels mounted on 17 of the 18 square panels. Each panel will contain 32 solar cells measuring  $2\text{cm} \times 4\text{cm}$  connected in series. This comprises an electrical string and the 17 electrical strings will be connected in parallel through a blocking diode to the electrical bus. There are two basic configurations - shunt and series - in which to meter the voltage and current levels in each panel.

#### **1. Shunt Method**

The solar cell parameter that is directly related to the incident angle of the sun's rays is  $I_{SC}$ . In order to obtain this measurement from the circuit it is necessary to electrically isolate the string from the bus and measure current at no load. This can be accomplished by adding a switch such that the current is shunted through a short from which current flow is metered. See Figure 5-6.

If the short is replaced with an infinite resistance,  $V_{OC}$  can be measured.  $V_{OC}$  varies logarithmically as a function of intensity and the resolution obtained is only  $30^\circ$ . This calculation is shown in Appendix A.

$I_{SC}$  measurement offers a more straight forward approach. The computer program developed by the Space System Academic Group which predicted effective surface area of PANSAT solar panels as it tumbled randomly was modified to provide the current levels for each panel at every sun angle. A panel current level will correspond to a sun incidence angle which will trace a circle of



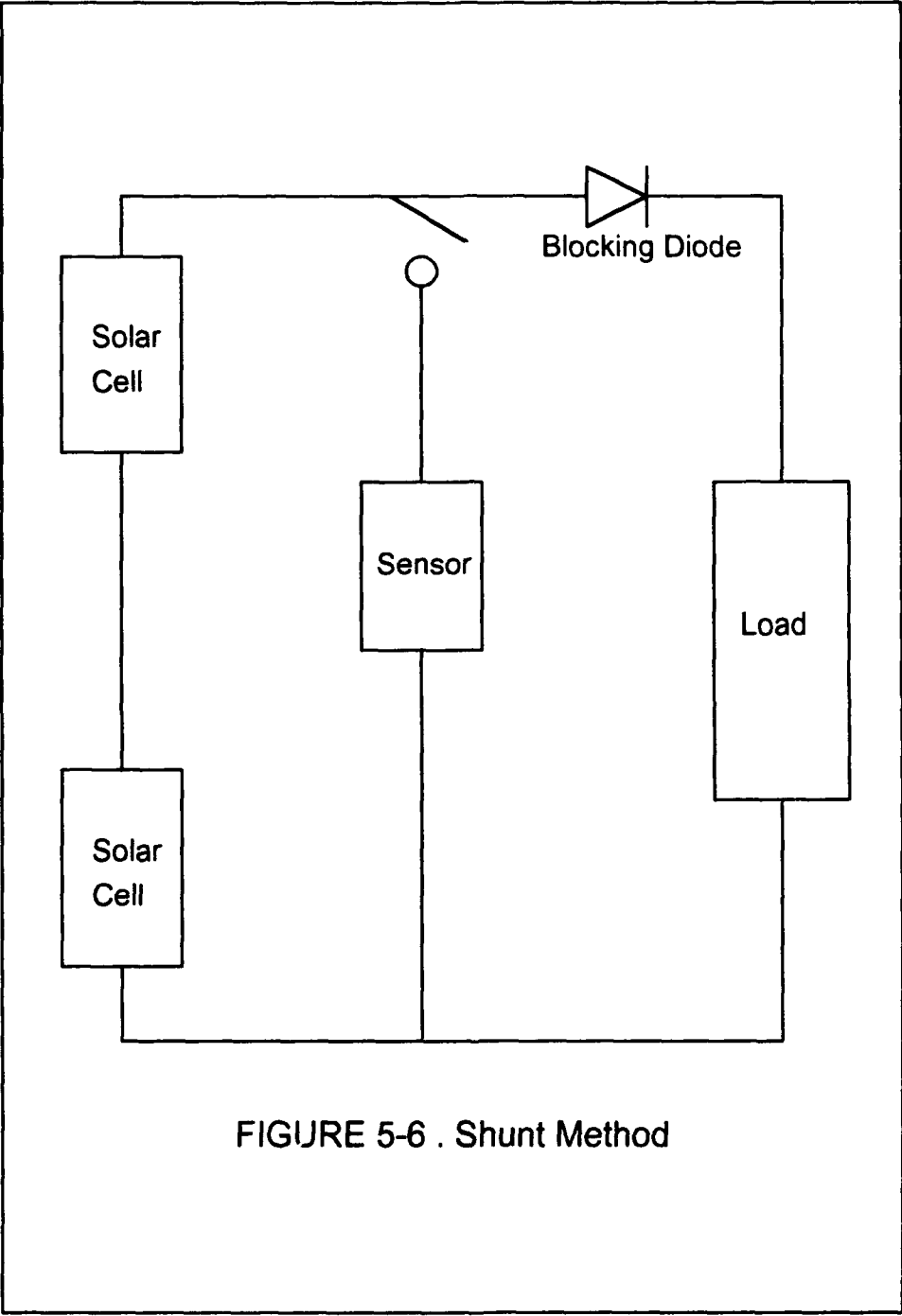


FIGURE 5-6 . Shunt Method

possible elevation and azimuth coordinates on PANSAT. To obtain specific elevation and azimuth coordinates enough panels must be sampled to provide a unique set of readings at each coordinate.

Not all 17 panels need to be sampled. A possible set of panels consist of the four panels adjacent to the triangular faces on the top and bottom half of PANSAT (eight panels total). Other combinations are also possible, however these eight panels offer the most symmetry. Other combinations are not as symmetric due to the use of the 18th square panel for the baseplate. The computer programs which generated the current database are in Appendix B.

*a. Resolution*

The maximum  $I_{SC}$  expected from each panel is not expected to exceed 360 mA. This includes  $I_{SC}$  increases due to solar constant fluctuations and 25°K rise in temperature. Using a 12 bit A/D converter, it will be possible to differentiate between 0.088mA current step sizes. This corresponds to a 1.27° resolution at the null point (  $\theta = 0^\circ$  ). The resolution becomes finer for angles greater the zero degrees.. This calculation is done in Appendix A.

*b. Accuracy*

Actual panel  $I_{SC}$  levels are correlated with predicted panel  $I_{SC}$  levels and thus sun angle coordinates can be derived. The accuracy of this sun sensor would depend on how accurately the current prediction model can compensate for fluctuations in  $I_{SC}$  due to temperature variations, solar flux intensity fluctuations, radiation degradation effects and albedo contributions.

$I_{SC}$  increases slightly with temperature - less than 1 percent per 10° K. However a one percent increase can cause as much as an 8° angle error.

Temperature of each panel is to be monitored in PANSAT, thus correction for temperature variation can be done.

The solar flux intensity depends on the sun earth distance and as a result varies with the earth's orbit. The solar flux intensity variation can be as great as 3.35 percent of the solar constant. However each panel will be affected in like manner.  $I_{SC}$  levels will increase proportionately in each panel. These values will still correlate with the prediction values.

Assuming each panel will encounter equivalent radiation doses and undergo uniform degradation, the effect of radiation degradation on  $I_{SC}$  will be the same for each panel.  $I_{SC}$  at EOL is expected to decrease to 98 percent of  $I_{SC}$  at BOL. [Ref. 17:p 51]

A definite bias ( as much as 30 percent increase) will be introduced by the albedo of the earth or moon. This will cause significant  $I_{SC}$  deviations. The prediction model must be able to anticipate the time when the albedo effects are present and filter out this bias from the  $I_{SC}$  panel readings.

*c. Sampling Frequency*

The expected tumbling rate of PANSAT is 0.1 rad/sec [Ref. 17:p. 13]. Thus each panel must be sampled at least twice this frequency. Photodiodes (structurally equivalent to solar cells but used in sensor applications ) are used for applications in which the frequency response requirements are below 1KHz. [Ref. 21] The minimum time to have sampled all the panels must be less than 1/1KHZ or one msec. This ensures that the time delay between sampling different panels is small enough to be considered instantaneous for the system.

## 2. Series Method

Voltage and current levels of the panel can be metered prior to the blocking diode. This configuration is shown in Figure 5-7. This method is more computationally intensive in that the voltage and current levels are determined not only by the illumination intensity incident upon the panel but also on load demand and battery charging / discharging activity.

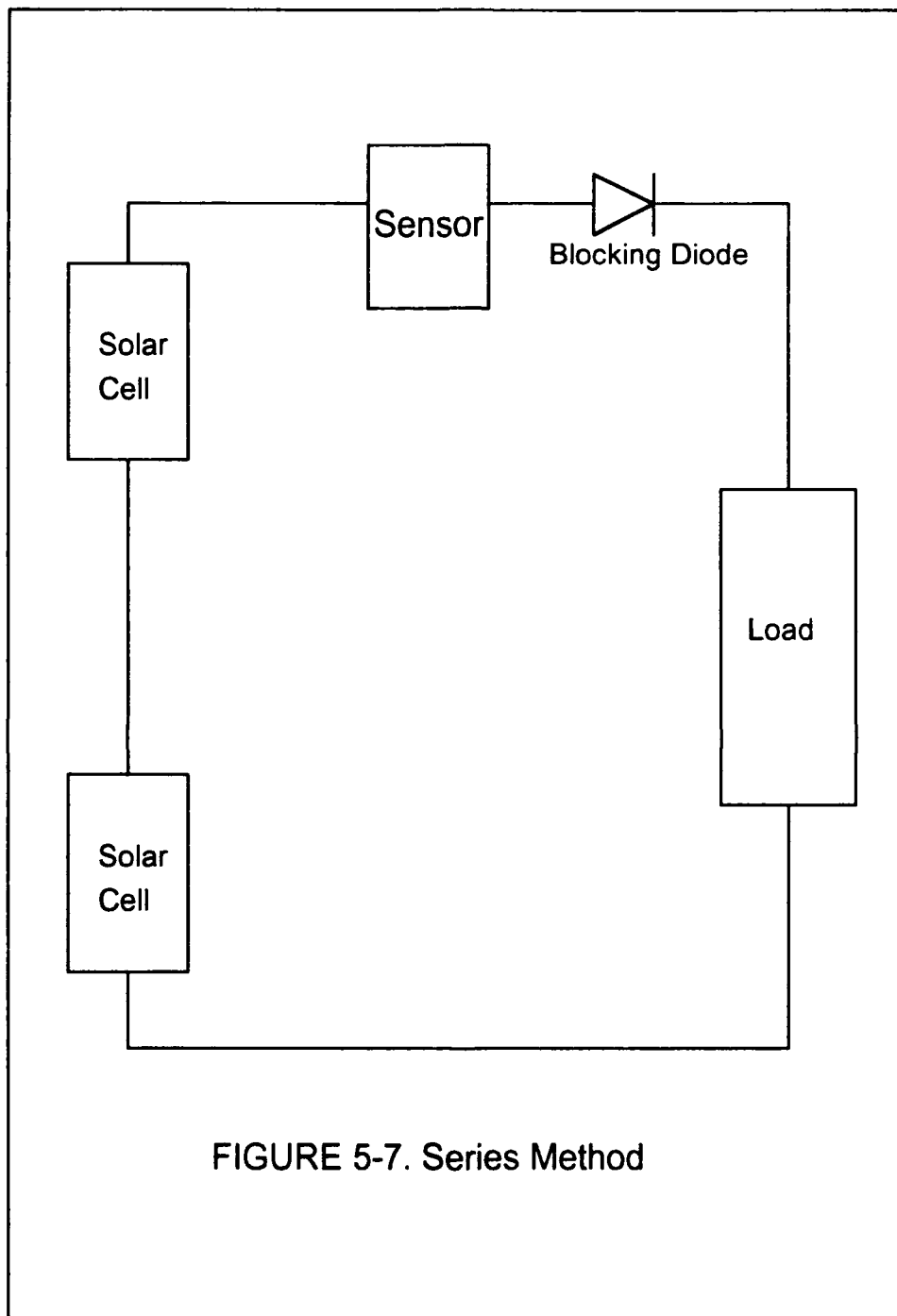
Algorithms which determine the power output of a panel and compare power levels between panels to ascertain sun orientation will be successful only if load demand is high enough such that all illuminated panels are able to contribute power to the bus. However this will not be the case at all times. Depending on the type of power conditioning / voltage regulation employed, at times of low load demand certain panels though illuminated will not be used by the system.

This is essentially a power flow problem. The power being supplied by the array panels must sum to equal the power consumed by the load and battery (the battery may be supplying power). Once the state of the electrical power system is determined, the operating point of each panel on a particular I-V curve can be found. This curve will yield a value for  $I_{SC}$  which maintains the link to the illumination incidence angle.

An extra dimension is added to the problem in that load behavior must also be considered. These load may not be purely resistive and may exhibit non linear properties. I-V curves must be obtained empirically for different load conditions. Transients (voltage and current surges) and noise may be introduced into the system during equipment startup, operation and shutdown. These must be considered in addition to compensating for parameter variations brought on by temperature, albedo etc as discussed in the shunt method.

This thesis did not obtain a prediction model using the series method. Design of PANSAT electrical power system had not yet defined specific loads to be able to simulate system operation.

The series method offers an advantage over the shunt method in that the array panels are not switched on and off the electrical bus. This switching would contribute harmonics to the system which may adversely impact certain loads. The disadvantage is that the voltage and current levels obtained are not a direct function of illumination incidence angle. Much computation is involved in order to yield  $I_{SC}$ .



## VI. CONCLUSIONS

Use of solar cells as a sensor for the sun is not a novel idea. They have been used in many types of commercial sun sensors. The terminal property to exploit is  $I_{SC}$ , which is a function of both illumination intensity and incidence angle. Unfortunately, when the solar cell is configured to yield this parameter, it cannot generate any useful power.

Solar cells in a power system are electrically connected in series and parallel to provide required voltage and current levels to a load. For PANSAT, each of the square panel arrays comprise a separate electrical string of solar cells which are connected in parallel through a blocking diode to the electrical bus. Thus power generated from one electrical string will provide an indication of the corresponding panel's orientation with respect to the sun. The symmetry and shape of PANSAT's structure readily provides a capability to triangulate a fix of the sun's location using the power signals from different panels.

However the power signals generated in the array do not have a direct dependence to the sun's orientation. To obtain this dependence, it would be necessary to electrically short the panel and measure  $I_{SC}$ . This is the shunt method described in Chapter V. Tables of expected values for  $I_{SC}$  are easily generated. This database is then used to compare with measured  $I_{SC}$  readings and sun orientation can be ascertained. The disadvantage of this method is that panels are switched from the bus in order to sample  $I_{SC}$ . This adversely affects power quality in that harmonics are created with the switching

Another approach, the series method, uses the voltage and current in the electrical string prior to the blocking diode. This will give the operating point on a particular I-V characteristic curve. Load conditions must be known for different load profiles will generate different I-V characteristic curves. Once the I-V characteristic curve is ascertained,  $I_{SC}$  can be found.

While both methods are valid solutions, the analysis must also consider ease of implementation and impact to the electrical power system. Both methods are computationally involved. Signals obtained ( current and / or voltage ) require processing to obtain sun orientation. Aging, thermal effects and bias due to earth and moon albedo will introduce error. This must be compensated for by software.

Compared to other power generating techniques, solar cells provide relatively low power output. Design of photovoltaic power systems for space applications is focused on optimizing solar cell performance and overall system efficiency. This especially applies for PANSAT's electrical power system. The design is limited by the available area onto which solar panels can be mounted. Use of a deployable array is not an option. Voltage and current sensors added to this system would require power for operation. Thus power allocated for housekeeping functions would have to increase. Note that most analog commercial sun sensors do not require input power.

Reliability is of paramount importance for the space power system designer. This translates to designs which minimize the number of parts and at the same time provides redundancy. With the implementation of a sun sensor, the complexity of the power system would increase and reliability would decrease.

Space power system designs evolve from an exhaustive iterative process in which each component is finely tuned so as to integrate with the whole system. It



is a design that is subjected to many constraints. To impose an additional requirement, such as a sun sensing capability, detracts from its primary function of power generation and distribution.

Solar cells can be used for sun sensing applications as well as for power generation. However these applications rely on different aspects of solar cell behavior. Solar cells configured for one application does not readily convert for use in the other application.

Therefore, it is recommended that the sun sensor not be implemented to PANSAT's electrical power system. Options such as mounting solar cells on the triangular panels of PANSAT should be investigated. These cells would be dedicated to sun sensing. Commercial sun sensor designs provide possible configuration schemes.

## APPENDIX A

### RESOLUTION CALCULATION FOR SHUNT METHOD

#### A. RESOLUTION USING $I_{SC}$ MEASUREMENT

	42.5mA/cm <sup>2</sup>	nominal $I_{SC}$
+	1.5 mA/cm <sup>2</sup>	solar constant fluctuation
+	1.0mA/cm <sup>2</sup>	25°K temperature rise
	<hr/>	
	45.0mA/cm <sup>2</sup>	
x	8 cm <sup>2</sup>	area of solar cell
	<hr/>	
	360 mA	maximum $I_{SC}$ per panel

Using a 12 bit A/D converter:

$$\frac{360}{2^{12}} = 0.088 \text{ mA} \quad \text{current step size}$$

$$\cos^{-1}\left(\frac{360 - 0.088}{360}\right) = 1.27^\circ$$

Resolution of  $1.27^\circ$  for  $I_{SC}$  at the null point (  $\theta = 0^\circ$  )

## B. RESOLUTION USING $V_{OC}$ MEASUREMENT

Given :

$$I_o = 3.4 \times 10^{-12} \quad \text{for } V_{OC} = 0.6V \text{ and } I_{SC} = 42.5mA$$

$$\frac{kT}{q} = 25.8 \text{ mV} \quad \text{at } T = 301^\circ K$$

$$\text{Maximum } V_{OC} = 0.6V/\text{cell} \times 32 \text{ cells} = 19.2V$$

Using a 12 bit A/D converter

$$\frac{19.2V}{2^{12}} = 0.0047V \quad \text{voltage step size}$$

From Equation 2-3

$$I_{SC} = I_o \left( e^{\frac{qV_{OC}}{kT}} - 1 \right)$$

$$V_{OC} = 0.6 - 0.0047 = 0.5953$$

$$I_{SC} = 3.4 \times 10^{-12} \left( e^{\frac{0.5953}{0.0258}} - 1 \right)$$

$$I_{SC} = 35.66 \text{ mA}$$

$$\cos^{-1} \left( \frac{35.66}{42.5} \right) = 32.95^\circ$$

Resolution of  $32.95^\circ$  for  $V_{OC}$  at null point (  $\theta = 0$  )

## APPENDIX B

### SHUNT METHOD PREDICTION PROGRAM

Figure B-1 is a schematic showing a 2 dimension topology of PANSAT. The square panels on PANSAT were assigned the following coordinates:

Panel 1	$(\hat{i})$	Panel 10	$\frac{1}{\sqrt{2}}(\hat{j} + \hat{k})$
Panel 2	$\frac{1}{\sqrt{2}}(\hat{i} + \hat{j})$	Panel 11	$\frac{1}{\sqrt{2}}(-\hat{i} + \hat{k})$
Panel 3	$(\hat{j})$	Panel 12	$\frac{1}{\sqrt{2}}(-\hat{j} + \hat{k})$
Panel 4	$\frac{1}{\sqrt{2}}(-\hat{i} + \hat{j})$	Panel 13	$\frac{1}{\sqrt{2}}(\hat{i} - \hat{k})$
Panel 5	$(-\hat{i})$	Panel 14	$\frac{1}{\sqrt{2}}(\hat{j} - \hat{k})$
Panel 6	$\frac{1}{\sqrt{2}}(-\hat{i} - \hat{j})$	Panel 15	$\frac{1}{\sqrt{2}}(-\hat{i} - \hat{k})$
Panel 7	$(-\hat{j})$	Panel 16	$\frac{1}{\sqrt{2}}(-\hat{j} - \hat{k})$
Panel 8	$\frac{1}{\sqrt{2}}(\hat{i} - \hat{j})$	Panel 17	$(\hat{k})$
Panel 9	$\frac{1}{\sqrt{2}}(\hat{i} + \hat{k})$		

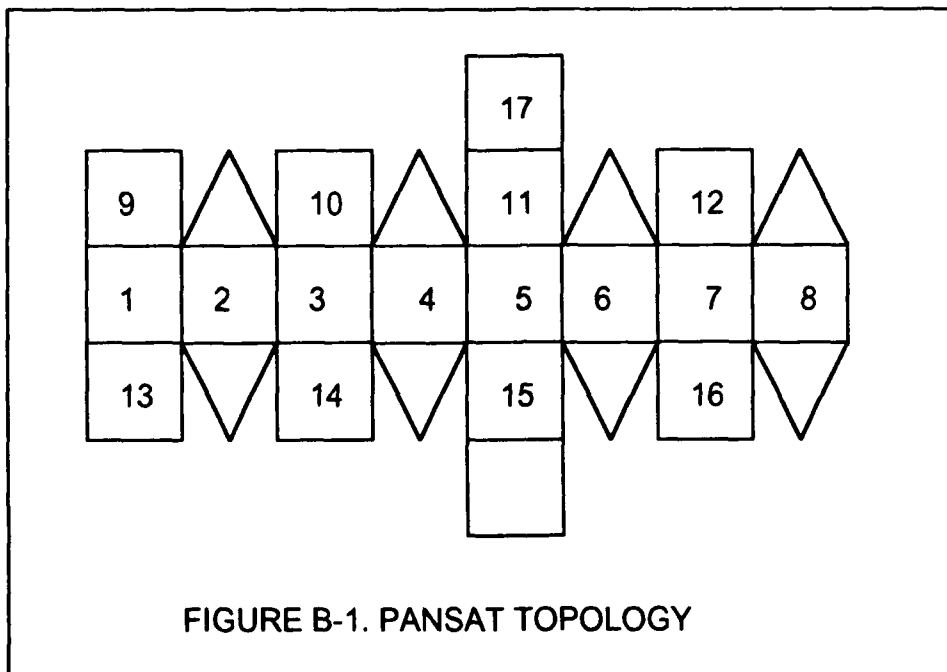


FIGURE B-1. PANSAT TOPOLOGY

The following MATLAB program generates predicted values for  $I_{SC}$  levels in a panel specified by the user. This data is calculated for 0 - 180° range in elevation angle and azimuth range of 0- 360°, thus covering the entire PANSAT sphere. Both angles are incremented in 1.2° increments. The data generated is then plotted.

```
% This program computes the short circuit current of a user specified
% solar panel array. The rotation angle about the Z-axis is varied 180 degrees
% and X-axis is varied 360 degrees. A mesh plot is then obtained.
%
clear;
clg;
Imax = 42.5                % nominal short circuit current (mA)

% The matrix S are the coordinates of the panels. The rows will give the x, y
% and z axis respectively. The columns give the panel number

S=[001 0.707 000 -.707 -001 -.707 000 0.707 0.707 000 -0.707 000 0.707 000 -0.707
000 000
000 0.707 001 0.707 000 -0.707 -01 -0.707 000 0.707 000 -0.707 000 0.707 000
-0.707 000
000 000 000 000 000 000 000 0.707 0.707 0.707 0.707 -0.707 -0.707 -0.707
-0.707 1];

panel= input('Enter the solar panel number (1-17): ');    %prompt user for panel

[theta,deg] = meshdom(0:1.26:180, 0:1.26:360);           %theta = elevation angle
                                                         %deg = azimuth angle

% Sun vector rotates counterclockwise in the x-y plane,(azimuth angle) starting
% at the y axis. Elevation angle is measured with respect to the x-y plane.

z=Imax*( -S(1,panel)*sin(theta*pi/180).*cos(deg*pi/180) ...
+ S(2,panel)*cos(theta*pi/180).*cos(deg*pi/180) ...
+ S(3,panel)*sin(deg*pi/180));

z0=find(z<=0);
z(z0)=zeros(z0);                %eliminate negative values, current will not
                                %flow in reverse due to blocking diode.

m=[260 40];                    %rotate graph so that azimuth angle is in front
mesh(z,m)
xlabel('Azimuth Angle (0-360 degrees)');

ylabel('Elevation Angle (0-180 degrees)');
```

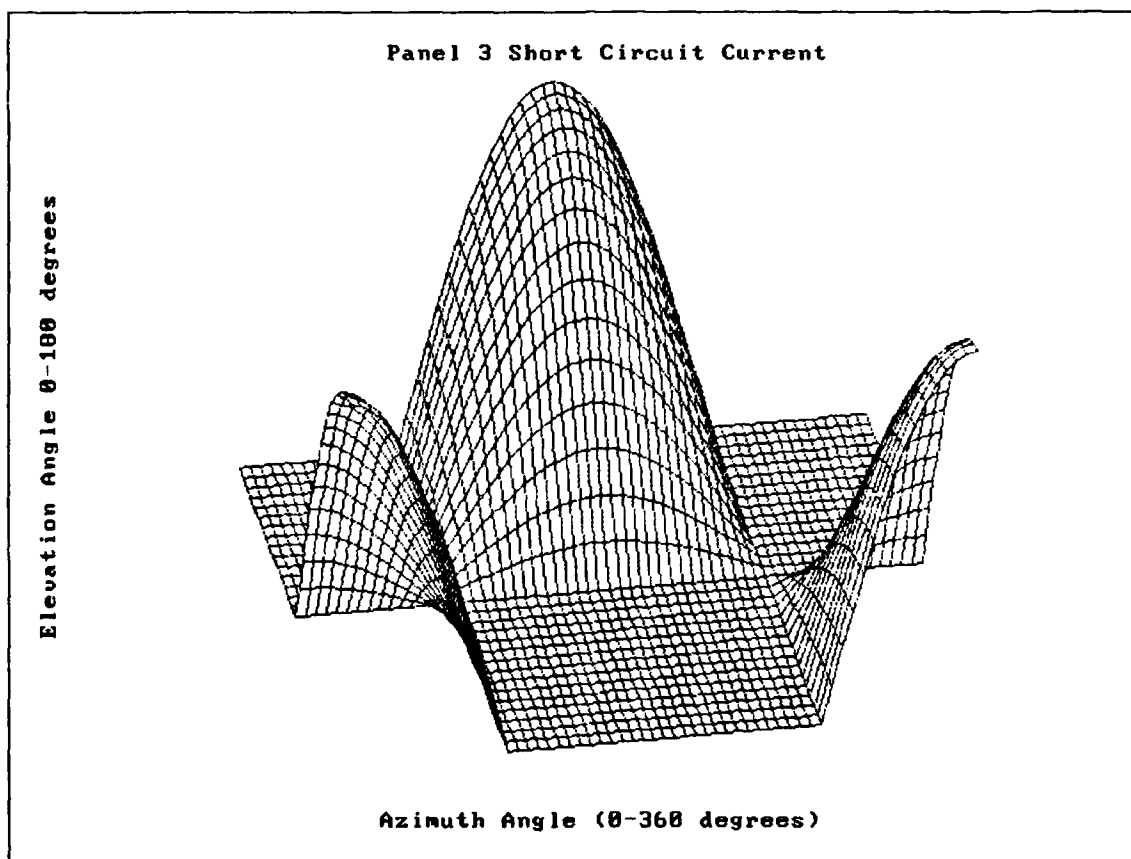


**Figure B-2. Plot of Short Circuit Current vs PANSAT Coordinates**

## LIST OF REFERENCES

1. Jet Propulsion Laboratory SP 43-38, *Solar Array Design Handbook*, v. 1, October 1976.
2. Rauschenbach, H. S., *Solar Array Design Handbook*, Van Nostrand Reinhold Co., 1980.
3. Iles, P. A., "Space Solar Cells - The Moving Target," *Proceedings of the 23rd Intersociety Energy Conversion Conference*, v. 3, 1989.
4. Sedra, A. S., and Smith, K. C., *Microelectronic Circuits*, 2d ed., Holt, Reinhart and Winston, 1987.
5. Chenming, H., and White, R. M., *Solar Cells From Basics to Advanced Systems*, McGraw - Hill Book Co., 1983.
6. Jet Propulsion Laboratory Publication 82-69, *Solar Cell Radiation Handbook*, 3rd ed., November 1982.
7. Green, M. A. , *Solar Cells Operating Principles, Technology, and System Applications*, Prentice - Hall Inc., 1982.
8. Becker-Irvin, C., "Solar Cell Reverse Biasing and Power System Design," *Proceedings of the 23rd Intersociety Energy Conversion Conference*, v. 3, 1989.
9. Cooley, W. T., "Air Force Photovoltaic Array Alternatives," *Proceedings of the 26th Intersociety Energy Conversion Conference*, v. 2, 1991.
10. Dakermanji, G., and Carlsson, U., "The Small Explorer Power System," *Proceedings of the 25th Intersociety Energy Conversion Conference*, v. 1, 1990.
11. Caldwell, D. J., Bavaro, L. T., and Carian, P. J., "Advanced Space Power System with Optimized Peak Power Tracking," *Proceedings of the 26th Intersociety Energy Conversion Conference*, v. 2, 1991.



12. Borger, W. U., and Massie, L. D., "Space Systems Requirements and Issues: The Next Decade," *Proceedings of the 25th Intersociety Energy Conversion Conference*, v. 1, 1990.
13. Hafen, D. P., and Corbett, R. E., "Cadmium Cell Cycle Life Prediction Equation for Low Earth Orbit," *Proceedings of the 16th Intersociety Energy Conversion Conference*, v. 1, 1981.
14. Yang, T. M., Keohler, C. W., and Applewhite, A. Z., "83 An Ni-H<sub>2</sub> Battery for Geosynchronous Satellite Applications," *Proceedings of the 24th Intersociety Energy Conversion Conference*, v. 3, 1989.
15. Moser, R. L., "Electrical Power Subsystem Initial Sizing," *Proceedings of the 25th Intersociety Energy Conversion Conference*, v. 2, 1990.
16. Space System Academic Group, Naval Postgraduate School, *Variation of PANSAT Power Due to Tumbling*, by D. Sakoda, 1989.
17. Noble, M. L., *Preliminary Design of the PANSAT Electrical Power Subsystem*, Master's Thesis, Naval Postgraduate School, Monterey, California, June 1990.
18. Space System Academic Group, Naval Postgraduate School, *PANSAT Functional Requirements*, 3 March 1992.
19. Space System Academic Group, Naval Postgraduate School, *Petite Amateur Navy Satellite (PANSAT) System Design Review*, present during design review held 19-20 May 1992.
20. Wertz, J. R., and others, *Spacecraft Attitude Determination and Control*, Kluwer Academic Publishers, 1978.

## INITIAL DISTRIBUTION LIST

	No. Copies
1. Defense Technical Information Center Cameron Station Alexandria, Virginia 22304-6145	2
2. Library, Code 52 Naval Postgraduate School Monterey, California 93943-5000	2
3. Chairman, Code EC Department of Electrical and Computer Engineering Naval Postgraduate School Monterey, California 93943-5000	1
4. Professor Rudolf Panholzer, Code SP/Pz Space Systems Academic Group Naval Postgraduate School Monterey, California 93943-5000	3
5. Professor Randy L. Wight, Code SP/Wt Space Systems Academic Group Naval Postgraduate School Monterey, California 93943-5000	1
6. Professor Edward Euler, Code SP/Eu Space Systems Academic Group Naval Postgraduate School Monterey, California 93943-5000	1
7. LT Irma Sityar 549 Kilimanjaro Drive Kissimmee, Florida 34758	1